
Masters Theses

Student Theses and Dissertations

Spring 2015

Development of a stochastic model for performance characterization of a PV/VRB microgrid

Kayla M. Speidel

Follow this and additional works at: https://scholarsmine.mst.edu/masters_theses



Part of the [Geological Engineering Commons](#)

Department:

Recommended Citation

Speidel, Kayla M., "Development of a stochastic model for performance characterization of a PV/VRB microgrid" (2015). *Masters Theses*. 7420.

https://scholarsmine.mst.edu/masters_theses/7420

This thesis is brought to you by Scholars' Mine, a service of the Missouri S&T Library and Learning Resources. This work is protected by U. S. Copyright Law. Unauthorized use including reproduction for redistribution requires the permission of the copyright holder. For more information, please contact scholarsmine@mst.edu.

**DEVELOPMENT OF A STOCHASTIC MODEL FOR PERFORMANCE
CHARACTERIZATION OF A PV/VRB MICROGRID**

by

KAYLA MARIE SPEIDEL

A THESIS

Presented to the Faculty of the Graduate School of the

MISSOURI UNIVERSITY OF SCIENCE AND TECHNOLOGY

In Partial Fulfillment of the Requirements for the Degree

MASTER OF SCIENCE IN GEOLOGICAL ENGINEERING

2015

Approved by

Dr. Curt Elmore, Advisor

Dr. Mariesa L. Crow

Dr. Norbert Maerz

PUBLICATION THESIS OPTION

The purpose of Sections 1-3 is to provide detail beyond what is presented in the journal manuscript which is included on pages 9-33. The purpose of Section 4 is to provide recommendations of future work with the model developed in this thesis. The paper in this thesis will be submitted as a journal article in the *International Journal of Smart Grid and Clean Energy*.

ABSTRACT

Photovoltaic (PV) Microgrids have been proven to be a useful technology in providing an environmentally friendly source of energy when compared to the use of fossil fuels. Accurately characterizing the performance of a microgrid system would ensure that the system is appropriately sized to meet electrical loads without a heavy reliance on diesel generators. A microgrid that is sized properly will reduce the cost of diesel fuel, while also reducing the risk of wasting money on an oversized system. A deterministic model which was created to characterize the performance of PV microgrids based on percent of time generator running was modified in order to perform a stochastic Monte Carlo analysis. The analysis used four random variables: global horizontal irradiance (GHI), ambient temperature, vanadium redox battery state of charge (VRB SOC), and energy load. Values for these variables in the model will be generated using PDFs derived from probability plots. Data for GHI and ambient temperature were taken from a TMY3 data set for the microgrid locations. Energy load data was collected over eight months and used to characterize the energy load for one year. The VRB SOC distribution was determined using engineering judgment. Three test methods will be performed on two microgrid systems to predict the performance of each system using stochastic and deterministic methods.

ACKNOWLEDGMENTS

I would like to thank Dr. Curt Elmore for motivating me throughout my research experience. He offered his guidance and support throughout the entirety of my thesis work. I would also like to thank my committee members Dr. Mariesa Crow and Dr. Norbert Maerz for their guidance and time.

I also want to acknowledge my great appreciation of Dr. Joe Guggenberger, Tu Nguyen, and Xin Qiu who were always willing to help me and answer questions. My office mates Dr. Yovanna Cortes Di Lena, Jessie Hahn, and Carlo Salvinelli also deserve special thanks for their support during my research.

I would like to thank my parents Tim and Deneen, my siblings Timmy and Stephanie, my sister-in-law Erin, my grandparents, and all the rest of my family and friends for always showing their support for furthering my education. Finally, I want to thank Michael for his motivation throughout my time as a graduate student. He made sure that I avoided becoming overstressed and was always there to encourage me.

TABLE OF CONTENTS

	Page
PUBLICATION THESIS OPTION.....	iii
ABSTRACT.....	iv
ACKNOWLEDGEMENTS.....	v
LIST OF ILLUSTRATIONS.....	viii
LIST OF TABLES.....	ix
SECTION	
1. INTRODUCTION	1
2. MODELING DESIGN AND WORK NARRATIVE	3
3. ORIGINAL CONTRIBUTION	8
PAPER	
Using TMY3 data to stochastically predict the performance of a PV/VRB microgrid..	9
ABSTRACT.....	9
1. INTRODUCTION.....	10
2. MICROGRID DESCRIPTIONS.....	13
2.1 Microgrid TA-246.....	13
2.2 Microgrid B2222.....	14
3. METHODS.....	15
3.1 GHI modeling.....	16
3.2 Ambient temperature modeling.....	19
3.3 VRB SOC modeling.....	21
3.4 Energy load modeling.....	22
3.5 Modeling process.....	24
4. RESULTS.....	26
5. CONCLUSIONS.....	30
NOTATION LIST.....	31
REFERENCES.....	32

SECTION	
4. RECOMMENDATIONS FOR FUTURE WORK.....	34
APPENDICIES	
A. PARAMETERS FOR STOCHASTIC VARIABLES.....	35
B. PROBABILITY AND DISTRIBUTION FITS.....	40
C. CORRELATION TABLES.....	44
BIBLIOGRAPHY.....	62
VITA.....	63

LIST OF ILLUSTRATIONS

	Page
Fig. 2.1. 5-Hour Load Profile for August 1, 2013.....	5
Fig. 2.2. Stochastic Analysis Trial Length Comparison.....	6
 PAPER	
Fig. 1. Microgrid Layout.....	14
Fig. 2. Ambient Temperature Trends for January.....	20
Fig. 3. Hourly Energy Load Profile for January 2014.....	23
Fig. 4. TA-246 Modeling Results.....	28
Fig. 5. B2222 Modeling Results.....	28
Fig. 6. Comparison of B2222 Modeling Results to Measured Performance.....	29

LIST OF TABLES

	Page
Table 1. P and Q Beta Parameters.....	19
Table 2. Ambient Temperature Trend Line Equations.....	21
Table 3. January Energy Load Parameters.....	24

1. INTRODUCTION

Photovoltaic (PV) microgrids are an advancing technology used to create self-reliant, renewable energy powered systems. A microgrid that is composed of energy storage and renewable energy generation components can alleviate the issues associated with fluctuations in renewable power supply. Barton and Infield (2004) state that storing excess renewable energy makes it accessible for later use when the renewable energy generated is insufficient to supply the load. Microgrids are useful in reducing the amount of fuel consumed by gasoline and diesel generators, and can be a cost effective method for providing electricity to off-grid locations. Modeling PV-microgrids is one way to increase the functionality of the systems. The models can be used to determine how often a site will be able to rely on renewable energy to provide energy, as well as how often a diesel generator will need to be used as a back-up method of energy production.

PV microgrids have several different components to their design. These components include the PV panels, inverters, charge controllers, and batteries. The PV panel component converts collected solar energy into direct current electricity with the use of semi-conducting materials. Inverters can be used to convert direct current electricity into alternating current electricity for other load uses. Charge controllers are installed to regulate the energy being stored in the battery component to prevent over charging and discharging. Batteries are used to store excess energy which is generated by the system for later use.

Variations that occur in ambient temperature and solar radiation globally due to changes in the location, weather, or season can affect the performance of a microgrid system. Ambient temperature, for example, has a direct relationship with the performance

of vanadium redox batteries (VRBs). The energy load associated with the system also affects performance. For renewable energy powered microgrids to be an effective energy source, proper sizing of the microgrid is necessary. A microgrid that is undersized will more heavily rely on the generator for energy production, therefore increasing the cost of energy. Over-sizing a microgrid in terms of PV and energy storage will produce sufficient energy to supply a load, but is not efficient in terms of capital cost.

2. MODELING DESIGN AND WORK NARRATIVE

The stochastic model designed in this thesis used the Guggenberger et al. (2012) model, which predicts the performance of a PV microgrid based on the operating time of a diesel generator using TMY3 data. Microsoft Excel was used as the spreadsheet based model software.

The addition of Oracle ® Crystal Ball to Microsoft Excel allowed for PV performance to be characterized using Monte Carlo simulations. The variables that were chosen to be modeled randomly included global horizontal irradiance (GHI), ambient temperature, VRB state of charge (SOC), and the energy load. In order to model these variables, data gathered from TMY3 data sets and field data were input into NCSS Statistical Software © Version 9.0.15 and Minitab ® 16 where the data were fit to probability density functions (PDFs). The PDF parameters were used to develop a Microsoft Excel based Monte Carlo model.

Daily averaged temperature values for ambient temperature were calculated for January and a trend line was fit to the data. The trend line showed no good fit to the daily averaged data with an R^2 value of 0.11. Hourly values for every day in the month of January were determined and the temperature trends for an average day were graphed. Three distinct trends became apparent in the graph. The temperatures for an average day were separated into three groups: cooling AM, warming, and cooling PM. The cooling period was separated into two categories due to a difference in the slope of the trend lines. R^2 values for the trend lines fit to the data sets yielded values of 0.97 for the cooling AM period, 0.90 for the warming period, and 0.94 for the cooling PM period. The trend line equations were used generate values of ambient temperature in the model.

A set of the values generated using the trend line equations were compared with the TMY3 values in the Ft. Leonard Wood dataset to ensure that the generated temperature values were identical. The data sets were compared to several different PDFs in order to determine the best fit for the simulation. Ambient Temperature was first compared to a normal distribution which yielded a P-value of 0.91 and was then compared to a lognormal distribution which gave a higher P-value of 0.96.

Based on the research conducted by Salameh et al. (1995) it was assumed that GHI data would fit a beta distribution. Salameh et al. (1995) compared several sets of TMY3 GHI data to Weibull, beta, and lognormal distributions to determine which would better model the data. Several different programs were used to fit GHI data to beta distribution. These programs included: NCSS Statistical Software © Version 9.0.15, XLSTAT Statistical Software Version 2014.1, and Minitab ® 16. NCSS Statistical Software © was determined to be the best choice for beta distribution fitting based on ease of use and user familiarity. After comparing the TMY3 GHI data set for the Ft. Leonard Wood site to the beta distribution it was ensured that the beta distribution is in fact the best fit to model GHI data.

The energy load was modeled from 8 months of collected data from site B2222. This data was recorded from two soda machines located inside. Figure 2.1 shows an example of the load data collected for a 5 hour period from 4 AM to 9 AM on August 1, 2013. In the figure, the two distinct frequencies of the machine loads can be seen. The HVAC component of the energy load was removed due to HVAC being incorporated into the PV model. The corrected data was used to create hourly datasets for each month, which were then fit to different PDF distributions. An attempt was made to fit energy

load data to distributions based on weekdays versus weekends, working hours versus non-working hours, and daily energy loads. However, no distribution was found to fit the data based on these groups. The hourly energy load data for each month was compared to both normal and lognormal distributions. Both showed good results, however, the lognormal distribution gave slightly better P-values, overall.

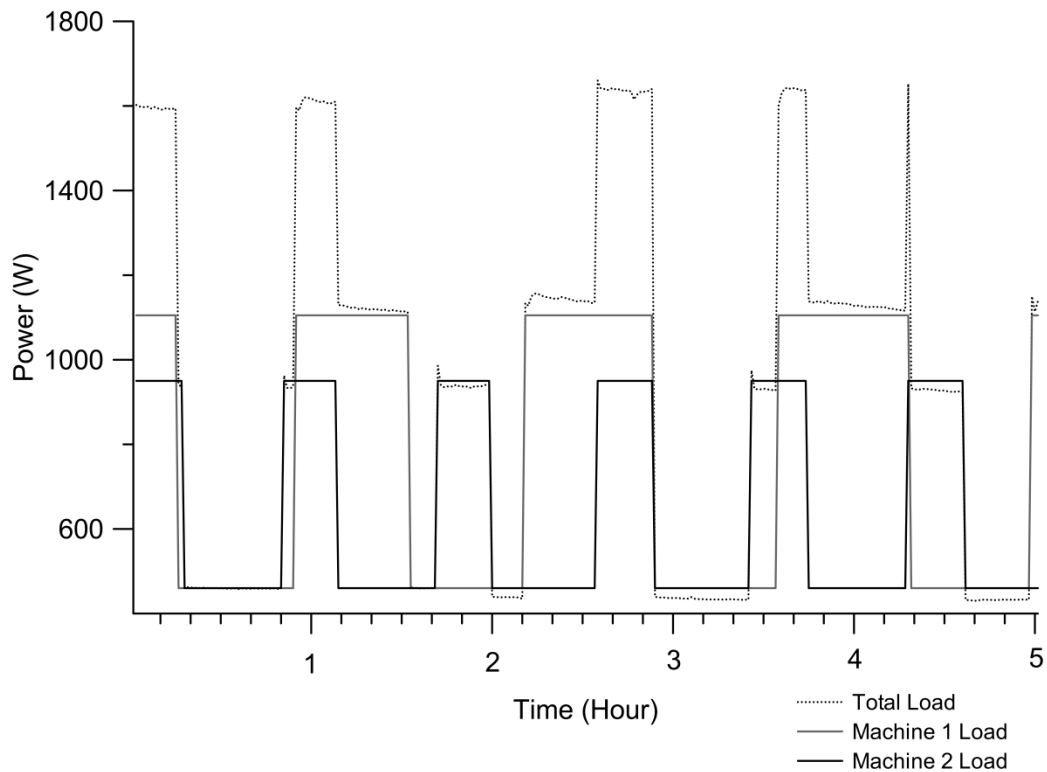


Fig. 2.1. 5-hour Load Profile for August 1, 2013

It was assumed that the VRB SOC follows a uniform distribution. In this case, the VRB SOC has an equal possibility of being anywhere from 6kW to 20kWh for microgrid TA-246 and 4kWh to 20kwh for microgrid B2222.

A sensitivity analysis was performed using 1,000 trials, 10,000 trials, and 100,000 trials to ensure the model results accurately represented the behavior of the system.

Figure 2.2 shows that modeling the system using 1,000 trials gave results identical to modeling using 100,000 trials. Therefore, to model the performance of the two microgrid systems 1,000 trials will be used.

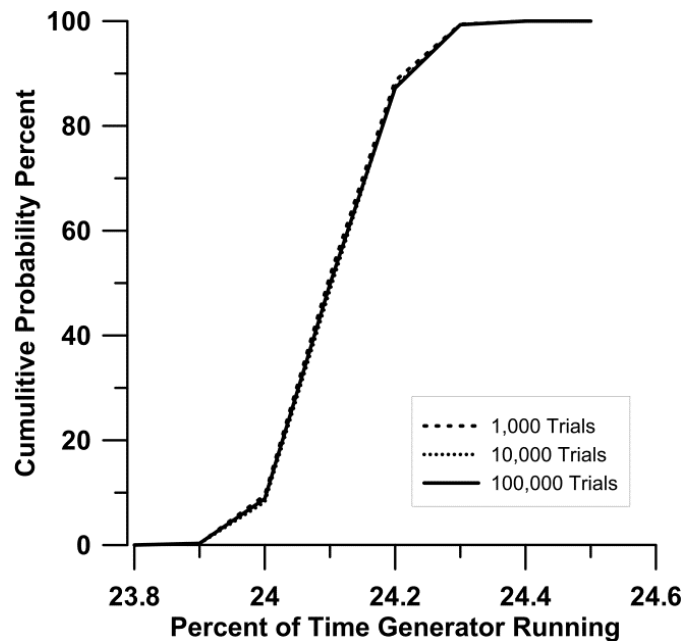


Fig. 2.2. Stochastic Analysis Trial Length Comparison

The model used in the simulation has several inputs. The characteristics of the PV systems that are input include the panel width (cm) and length (cm), the number of panels, and the array efficiency. The step length (min), inverter efficiency, sensor load (watts), generator power ranking (kW), generator starting SOC (V) and ending SOC (V) are also input.

Parasitic loads such as HVAC were accounted for based on the ambient temperature. The correlation between the HVAC and ambient temperature was studied. Modeling HVAC as a pure function of ambient temperature yielded an R^2 value of 0.63. It was determined that to reach a higher R^2 value more information would need to be included into the model. Additional information could include wind speed, barometric pressure, and VRB temperature. Due to time constraints, it was assumed that HVAC and ambient temperature have a perfect correlation in this model. The HVAC system ran more often in the summer months to keep the VRBs cool and less often during the winter months when temperatures were low.

The model output the frequency that the diesel generator was on and off for each month which was calculated as a percent. The time when the generator was off is the time when the system was operating fully on renewable energy. Therefore the renewable operating percent can be determined simply by subtracting the generator operating percent from 100 percent.

3. ORIGINAL CONTRIBUTION

The objective of this research was to develop a stochastic model with Microsoft Excel that will provide reasonable predictions on the performance of a PV microgrid based on the operating time of a connected diesel generator. Guggenberger et al. (2012) previously modeled PV systems had been achieved with a deterministic approach using Microsoft Excel. The deterministic model was able to accurately characterize the performance of microgrids, but did not take into account the variability that can occur with environmental conditions. The model in this thesis was designed to characterize the range of performance for a PV system which can be more realistic due to the variable nature of factors such as GHI, ambient temperature, VRB SOC, and energy load.

The original contribution of this thesis is the applicability of TMY3 datasets to generate GHI and ambient temperature PDFs for the purpose of stochastically predicting the performance of PV/VRB microgrids.

PAPER

Using TMY3 data to stochastically predict the performance of a PV/VRB microgrid

Kayla M. Speidel¹, A.C. Elmore, Ph.D., P.E.² and Joe D. Guggenberger, Ph.D., P.E.³

Authors

¹Graduate student, Department of Geological Engineering, Missouri University of Science and Technology, 1400 N. Bishop Ave., 124 McNutt Hall, Rolla, MO 65409; PH (573) 341-6957; FAX (573) 341-6953; email: kms5y2@mst.edu

²Professor of Geological Engineering, Missouri University of Science and Technology, 1400 N. Bishop Ave., 124 McNutt Hall, Rolla, MO 65409; PH (573) 341-6957; FAX (573) 341-6953; email: elmoreac@mst.edu

³Assistant Professor of Geological Engineering, Missouri University of Science and Technology, 1400 N. Bishop Ave., 318 McNutt Hall, Rolla, MO 65409; PH (573) 341-4466; FAX (573) 341-6953; email: jguggenb@mst.edu

ABSTRACT

Accurately characterizing the performance of an off-grid photovoltaic (PV) microgrid system can help ensure that the system is appropriately sized to reduce the reliance on supplemental power generation via diesel-fueled generators. However, deterministic models cannot account for the inherent variability of solar insolation, ambient temperature, initial battery charge, and electrical load. A Monte Carlo model was

developed by identifying those four variables as random variables. Typical Meteorological Year 3 (TMY3) data were used to develop the probability density functions (PDFs) for the environmental variables, and the initial charge PDF was developed using engineering judgment while the load PDF was based on observed data. Comparison of the stochastic model results against limited performance data from two PV-based microgrid systems with vanadium redox batteries in Missouri indicated that the stochastic technique has the potential for widespread applicability. This potential is due in part because TMY3 datasets are available throughout the United States, and the basic model may be modified to include energy storage systems other than the subject vanadium redox battery.

1. INTRODUCTION

Electrical microgrids are systems that can be used to increase the efficiency of power delivery to neighborhoods or areas that are typically served by utility companies as discussed by Provata et al. and Patterson et al. (2014), or they are systems that are used to provide power to locations that do not have access to utility -provided power such as those described by Merei et al. (2013) and Bandara et al. (2012). This paper addresses the second category of microgrids, specifically those that use a combination of renewable energy sources such as photovoltaic (PV) to produce power, back-up diesel-powered generators, and batteries to store energy. Fossati et al. (2004) describe how the design of such a microgrid balances the capital costs associated with the PV component and the

battery component with the operating costs associated with a fossil-fuel generator for an expected electrical load profile. Performance prediction models are used to estimate the operational frequency of the fossil-fuel generator considering the environmental conditions such as solar insolation and ambient temperature that are variables in the production of PV power. Those environmental factors may also impact the operational efficiency of the energy storage devices. For example, vanadium redox batteries (VRBs) and other batteries are impacted by ambient temperature (Guggenberger et al. 2012).

Several models have been developed to model these systems. Guggenberger et al. (2012) created a microgrid performance model which characterized the performance of a PV/VRB microgrid based on the operation of a backup diesel generator. This deterministic model used typical meteorological year 3 (TMY3) data for the global horizontal irradiance (GHI) and temperature input values for a microgrid located at Fort Leonard Wood in Pulaski County, Missouri. The model produced reasonable results, but it did not account for the inherent randomness in the environmental and load variables used in the calculations.

Arabali et al. (2014) describe the development of a stochastic model that uses Monte Carlo simulation (MCS) methods to simulate a PV and wind-turbine powered system with energy storage to supply a deferrable heating ventilation and air conditioning (HVAC) load. Their work used case studies to show the usefulness of their approach at the electric utility service scale. Others including Kishore and Fernandez (2011) and Khatod et al. (2010) have used MCS to simulate the performance of PV and wind-based

microgrids, but those efforts have typically assumed traditional lead-acid or similar energy storage components.

This paper describes the development of a MCS model based on the Guggenberger et al. (2012) deterministic model for a PV/VRB microgrid. The model includes four random variables: GHI, ambient temperature, VRB state of charge (SOC), and energy load. The stochastic analysis was performed for two microgrid systems, called TA-246 and B2222, located at Fort Leonard Wood. The probability density functions for GHI and ambient temperature were developed from typical meteorological year 3 (TMY3) data for that location. Three different initial VRB SOC conditions were evaluated: operating the microgrid for one year with a single randomly generated initial SOC at day one; operating the microgrid for one year with a unique initial SOC randomly generated at the beginning of each month, and operating the microgrid for one year where the initial SOC was charged to the upper threshold percent at the beginning of each month. These scenarios were used to evaluate three different system commissioning strategies: the system operated automatically for a year; the system operated automatically for single months; and the VRB was manually recharged at the beginning of each month.

2. MICROGRID DESCRIPTIONS

2.1. Microgrid TA-246

Microgrid TA-246 was constructed at a forward operating base (FOB) training area at Fort Leonard Wood, Missouri. The location latitude is 37.71 degrees and longitude is -92.15 degrees. The following system description is summarized from Guggenberger et al. (2012). The microgrid consisted of a 6 kW PV array that included 30 - 200 W Brightwatts Inc. solar panels (model BI-156-200W-G27V). The PV system was separated into two 3 kW arrays and was mounted with a fixed horizontal angle of 38 degrees facing due south. The panels were connected to two Outback FlexMax 80 charge controllers that were used to charge a nominal 38-cell Prudent Energy 5kW VRB with a rated energy density of 20 kWh. A three-cylinder Kubota diesel engine was connected to a Leroy Somer 8 kW brushless self-regulated generator. The generator was connected to the VRB using a Xantrex DC/AC inverter charge controller, and the system was controlled to minimize the use of the diesel-powered generator. Figure 1 shows a schematic of microgrid TA-246.

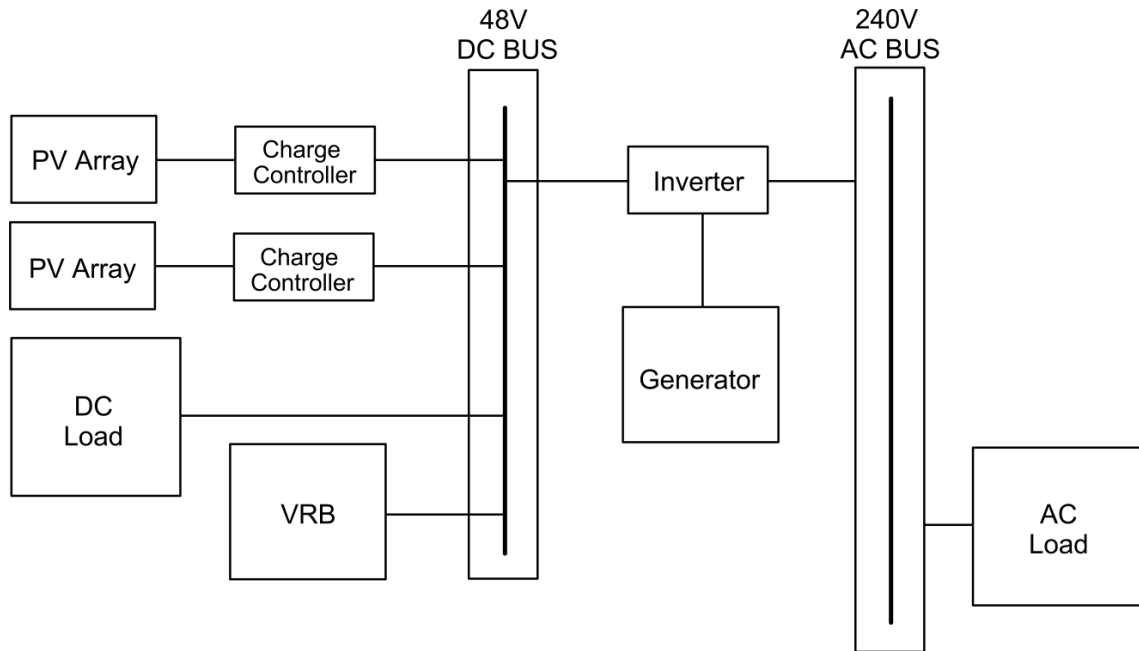


Fig. 1. Microgrid Layout

2.2. Microgrid B2222

Microgrid B2222 was constructed at a site at Fort Leonard Wood, MO at latitude 37.71 degrees and longitude -92.15 degrees. The following system description is summarized from Nguyen et al. (2013). The microgrid consisted of a 15 kW PV array which included 54 - 280 W Suntech solar panels (model STP280-24/Vd). The system was separated into three 5 kW arrays and was mounted with a fixed horizontal angle of 38 degrees facing due south. The array was connected to three Outback FlexMax 80 charge controllers which were used to charge a 38-cell Prudent Energy 5kW VRB with a rated energy density of 20 kWh. The system supplied power to a nearby building load when the microgrid (PV and/or VRB) had sufficient power to satisfy the load. If there was insufficient renewable resources available, a transfer switch was flipped and the building operated on the utility grid. The VRB was only charged by the PV arrays, but the

stochastic analyses presented in this paper were performed by assuming that that microgrid included the previously described three-cylinder Kubota diesel engine with a Leroy Somer 8kW brushless self-regulated generator.

3. METHODS

The random variables used in the model included GHI, ambient temperature, initial VRB SOC, and energy load. The U.S. Department of Energy's National Renewable Energy Laboratory (NREL) maintains the National Solar Radiation Database (NSRDB) which is a ready source for hourly data including irradiance, ambient temperature, and wind speed for over 1,000 locations across the United States. Wilcox and Marion (2008) state that typical meteorological year (TMY) data sets hold hourly values of solar radiation and meteorological elements for a 1-year period. They are intended to be used for computer simulations of solar energy conversion systems and building systems for performance comparisons of different system types, configurations, and locations in the United States and its territories. Wilcox and Marion (2008) go on to describe a TMY data set as being composed of 12 typical meteorological months (January through December) that are concatenated essentially without modification to form a single year with a serially complete data record for primary measurements. The monthly data sets contain actual time-series meteorological measurements and modeled solar values, though some hourly values may contain filled or interpolated data for periods when original observations are missing from the data archive.

3.1. GHI modeling

Salameh et al. (1995) fit hourly solar irradiance data to Weibull, lognormal, and beta PDFs in order to describe the randomness of solar radiation. They used chi-squared and Kolmogorov-Smirnov testing to show that for a majority of the hourly data groups, a beta distribution function yielded the best goodness of fit results. Solar irradiance was also assumed to follow a beta distribution to provide the available solar power in source in Karaki et al. (1999). Therefore this study used beta PDFs to simulate GHI. The GHI beta distribution parameters were calculated from the closest TMY3 dataset, Fort Leonard Wood Army Air Field (AAF) (TMY 724457) to the subject microgrid locations. A TMY3 dataset consists of 8,760 lines which correspond to the 8,760 hours in a year beginning at 1 AM on January 1st and ending on 12 AM on December 31st. For each dataset line, the GHI value is the total amount of direct and diffuse solar radiation received on a horizontal surface during the corresponding 60-minute time period (Wilcox and Marion, 2008). Therefore GHI values for TMY3 dataset lines that include sunrise or sunset are for a fraction of an hour and are not appropriate for use in the Guggenberger et al. (2012) model which requires hourly values.

The TMY3 extraterrestrial radiation normal (ETRN) data were used to determine if the first and last value of GHI recorded for each day was representative of a full hour of sunlight. Wilcox and Marion (2008) define ETRN as the amount of solar radiation in Wh/m² received on a surface normal to the sun at the top of the atmosphere, and those values are typically on the order of 1,400 Wh/m² for a full hour of sunlight for the subject TMY3 station. When the first and/or last ETRN values for a day were lower than the

other values for that day, the first and/or last GHI measurements for that day were not retained.

The GHI values were normalized for the PV array geometry angle of incidence and corresponding pointing error. Pointing error was determined by first calculating the solar altitude angle for each hour using the equation given by Masters (2013) using location latitude (L), solar declination (δ), solar hour angle (H), and the day number (n):

$$\beta = \sin(L) \sin(\delta) + \cos(L) \cos(\delta) \cos(H) \quad (1)$$

where

$$\delta = 23.45 \sin \left[\frac{360}{365} (n - 81) \text{deg} \right] \quad (2)$$

Pointing error was calculated using equation (3). The GHI values were then normalized by dividing each retained hourly value by its corresponding pointing error. The normalized GHI values were then separated by month, and then grouped according to hour.

$$\textit{pointing error} = \sin(\beta) \quad (3)$$

Ang and Tang (1975) state that the beta distribution is appropriate for a describing random variable whose values are bounded between a maximum and minimum using the

two shape parameters (P and Q) and two parameters representing the minimum (A) and the maximum (B). Those authors give the beta PDF as a function of time (t) as:

$$f(t) = \frac{1}{B(P,Q)} \frac{(t-A)^{(P-1)}(B-t)^{(Q-1)}}{(B-A)^{(P+Q-1)}}, P > 0, Q > 0, A < t < B \quad (4)$$

where

$$B(P, Q) = \frac{\Gamma(P)\Gamma(Q)}{\Gamma(P+Q)}$$

All of the normalized GHI values for each full hour of sunlight for every month were assembled into a single dataset, and A , B , P , and Q were calculated for each using NCSS Statistical Software 9.0.15. Table 1 lists the beta distribution parameters P and Q for each hour every month. Strong positive correlations from hour to hour in GHI were found using Minitab ® 16. Correlations showed a high probability of a large GHI value occurring in a given hour if the previous hour also yielded a large GHI value. Correlation values ranged from 23 percent to 94 percent with a mean of 77 percent. These correlations were included in the model.

Month	Parameter	Hour											
		7	8	9	10	11	12	13	14	15	16	17	18
Jan	P				1.2	0.71	1.3	0.79	4.7	2.2			
	Q				1.0	0.31	1.6	1.2	11	2.3			
Feb	P				1.8	1.4	2.0	2.9	2.9	5.3			
	Q				1.9	1.0	1.5	2.8	2.2	4.8			
Mar	P			0.86	0.59	0.98	0.92	1.7	1.0	1.3			
	Q			1.4	0.46	1.5	1.9	3.3	1.6	2.3			
Apr	P		1.5	1.2	1.4	2.2	1.7	2.3	3.2	2.8	3.0	3.0	
	Q		2.5	1.3	1.4	2.5	1.5	1.9	3.4	2.2	3.3	2.8	
May	P		4.6	3.1	1.2	1.6	4.9	2.1	3.5	2.7	2.4	1.4	1.5
	Q		5.5	0.75	0.3	1.1	3.6	1.4	1.1	1.1	0.6	0.6	1.1
Jun	P	4.9	3.9	3.3	2.2	1.6	1.5	1.9	2.0	2.5	1.9	1.6	3.0
	Q	7.6	3.2	1.5	0.95	0.83	0.86	0.89	1.4	1.9	1.1	0.79	2.0
July	P		8.2	7.3	5.7	5.2	2.1	2.5	3.7	1.6	1.7	2.8	3.9
	Q		5.9	2.5	0.89	0.83	0.5	0.8	1.2	0.78	0.4	0.63	0.61
Aug	P		3.5	2.6	1.4	1.5	2.0	2.1	4.3	4.3	2.2	4.7	
	Q		4.8	1.8	0.53	0.59	1.4	1.3	2.0	2.4	0.87	1.4	
Sep	P			1.8	1.3	1.1	3.3	1.6	3.5	1.3	1.8	2.2	
	Q			1.2	0.65	0.86	3.9	1.2	3.7	0.92	1.2	1.8	
Oct	P			1.1	0.95	0.90	0.93	0.94	0.82	1.3	2.4		
	Q			0.85	0.50	0.54	0.66	0.52	0.54	1.0	1.1		
Nov	P				1.2	1.7	1.5	1.9	1.4	1.4	1.7		
	Q				1.6	2.4	1.9	2.6	1.5	1.5	1.8		
Dec	P				1.5	1.3	1.5	1.5	1.7	1.9	2.5		
	Q				1.8	1.1	1.4	1.4	1.5	1.6	1.9		

Table 1. P and Q Beta Parameters

3.2. Ambient temperature modeling

Ambient temperature ($^{\circ}\text{C}$) was modeled from TMY3 data for Fort Leonard Wood based on the time of day for each month. For each day, data was broken down into three categories: morning cooling, warming, and evening cooling. The cooling period was separated into two categories due to different trends in the data that are shown in the Figure 2 example. Ambient temperature trends were created for all 12 months. A probability plot analysis showed that the data fit a lognormal PDF where the conditional shape was given by the equation of the trend line. These equations and the corresponding

shape and scale factors are listed in Table 2. Strong positive correlations from hour to hour in ambient temperature were also found using Minitab ® 16. Correlations showed a high probability of a high temperature occurring in a given hour if the previous hour also had a high temperature, and the same with low temperatures. Correlation values ranged from 73% to 100% with an average of 97%. These correlations were included in the model.

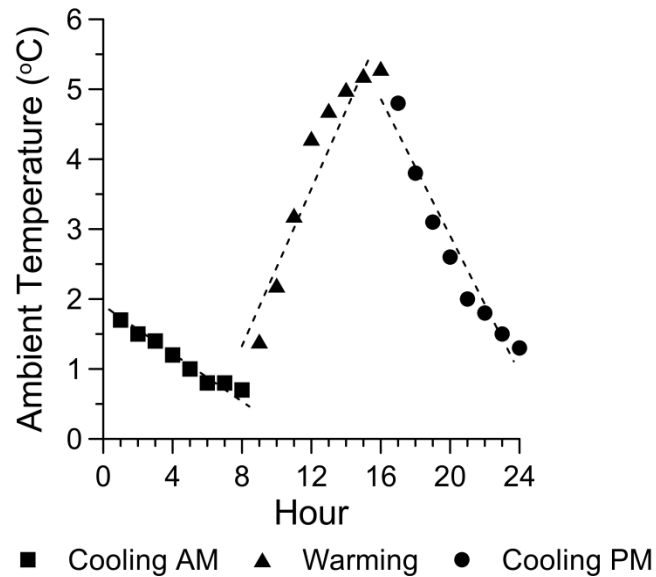


Fig. 2. Ambient Temperature Trends for January

Month	Cooling AM (y (°C) =)	Warming (y (°C) =)	Cooling PM (y (°C) =)
January	$-0.149x + 1.81$	$0.573x + 1.34$	$-0.482x + 4.782$
February	$-0.271x + 2.75$	$0.968x + 3.21$	$-0.739x + 8.34$
March	$-0.148x + 4.34$	$0.498x + 5.54$	$-0.441x + 8.68$
April	$-0.214x + 8.89$	$0.956x + 9.26$	$-1.01x + 16.6$
May	$-0.500x + 15.5$	$1.33x + 15.7$	$-1.17x + 25.0$
June	$-0.387x + 22.1$	$1.04x + 21.9$	$-0.907x + 29.4$
July	$-0.529x + 24.2$	$1.34x + 23.3$	$-1.08x + 32.5$
August	$-0.250x + 21.0$	$0.941x + 22.8$	$-0.941x + 28.7$
September	$-0.339x + 16.8$	$1.05x + 17.1$	$-0.847x + 23.5$
October	$-0.214x + 13.9$	$1.16x + 14.8$	$-1.05x + 21.4$
November	$-0.195x + 3.60$	$0.466x + 3.49$	$-0.323x + 6.09$
December	$-0.194x + 1.46$	$0.558x + 1.60$	$-0.411x + 4.46$

Table 2. Ambient Temperature Trend Line Equations

3.3. VRB SOC modeling

Nguyen et al. (2013) described VRBs as a flow-type battery that stores chemical energy and produces electricity using reduction-oxidation (redox) reactions between vanadium in the electrolytes. The batteries include two closed electrolyte circuits where, in each circuit, the electrolyte is stored in a separate tank and circulated through the cell stacks where the electrochemical reactions take place. Nguyen et al. (2013) also state that charge and discharge operations of a VRB are dependent on the SOC, the energy load, and the power produced by the PV array. During the discharge stage of operations, the VRB supplies power to the energy load, and pumps within the VRB. During the charging stage of operation, the pumps within the VRB cycle the electrolytes stored in the tanks through the cell stacks. VRB capacity changes due to the amount of energy going in and out of the system at any given time. Therefore VRB SOC can be determined from the capacity using the Guggenberger et al. (2012) equation:

$$VRB\ SOC = \left[\frac{9}{20} \left(VRB\ Capacity + \frac{10}{9} \right) \right] \quad (5)$$

The VRB energy capacity for the system at TA-246 was a maximum of 20 kWh. The VRB initial SOC was assumed to fit a uniform PDF. The lower threshold of the PDF was assumed to be 30 percent of the overall maximum charge, while the upper threshold for the distribution was chosen to be 80 percent of the overall maximum charge. The lower threshold was chosen because at a charge of 30 percent, the system switches from running off of the VRB to running on the generator. The upper threshold of the VRB charge capacity was chosen because once the VRB is re-charged to at least 80 percent, the system then switches back to running off the VRB (Guggenberger et al. 2012). The uniform distribution for the VRB SOC has a minimum value of 6kWh and a maximum value of 20kWh.

The B2222 microgrid used similar SOC thresholds except that the lower threshold was assumed to be 20 percent of the overall maximum charge and the upper threshold was assumed to be 73 percent in order to be consistent with the system described in Nguyen et al. (2013). The uniform distribution for the VRB SOC for this system has a minimum value of 4kWh and a maximum value of 14.6kWh.

3.4. Energy load modeling

Eight months of energy load data were available from the B2222 office building, and those data were used to develop the load PDF. An example of the energy load over a one-month period is shown in Figure 3. The collected monthly energy load data

generally ranged between 480-1,500 kWh, with higher energy load demands occurring in the summer months. The load data were compiled into hourly groups ranging from 1AM to 12AM, each hourly data set fit a lognormal distribution.

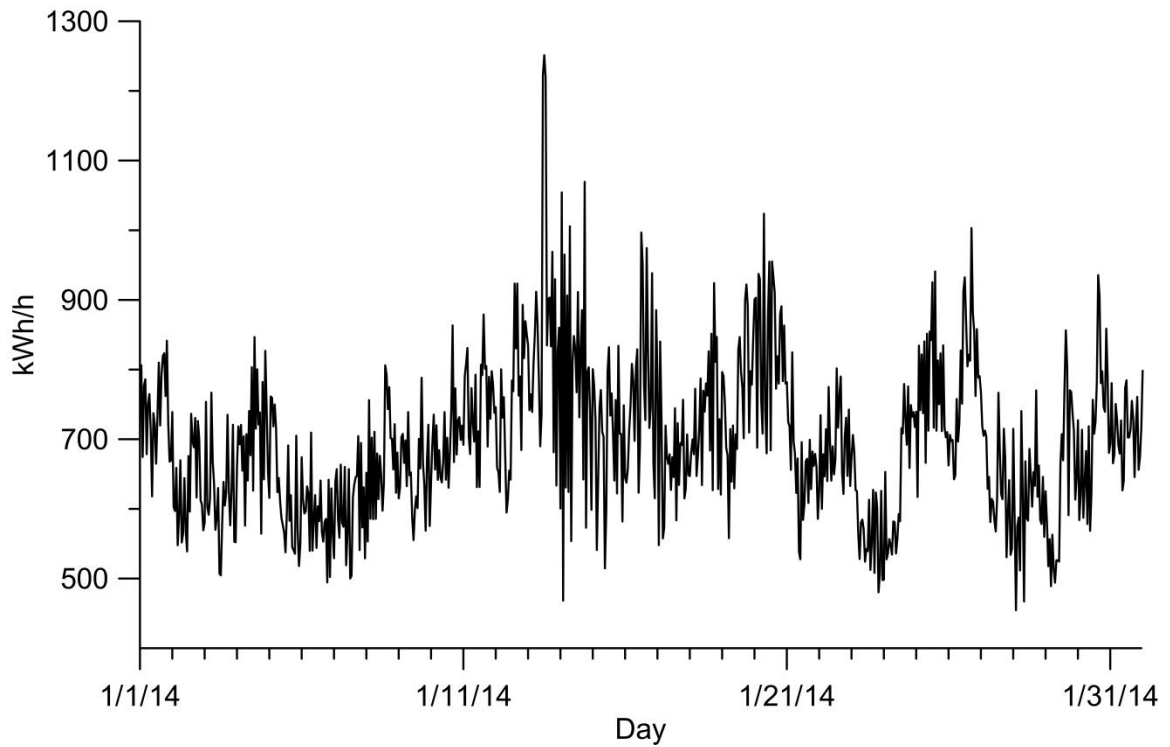


Fig. 3. Hourly Energy Load Profile for January 2014

Parameters determined from the lognormal probability plots were used to generate PDFs to predict the values of energy load at any given hour. Examples of the parameters used for the energy load during January are shown in Table 3.

Hour	Location	Scale
1	6.54	0.146
2	6.50	0.112
3	6.52	0.114
4	6.51	0.111
5	6.50	0.141
6	6.52	0.173
7	6.51	0.104
8	6.48	0.101
9	6.46	0.121
10	6.48	0.094
11	6.53	0.204
12	6.54	0.185
13	6.59	0.151
14	6.59	0.137
15	6.60	0.166
16	6.60	0.165
17	6.58	0.137
18	6.58	0.158
19	6.54	0.217
20	6.58	0.171
21	6.53	0.139
22	6.53	0.130
23	6.50	0.152
24	6.53	0.150

Table 3. January Energy Load Parameters

3.5. Modeling process

Microgrids TA-246 and B2222 were modeled to operate in either *renewable* mode or in *diesel* mode based on the modeled VRB SOC.

1. *Renewable mode.* This mode operated when the energy load was powered by the VRB and the available PV systems power. The microgrid was renewable mode when

the VRB SOC greater than the lower threshold SOC, or when the PV power was sufficient to both charge the VRB and supply power to energy load.

2. *Diesel mode.* When the VRB was in discharging stage and the SOC was lower than the lower threshold SOC, the system switched to *diesel* mode. This mode operated when the energy load was powered by a three-cylinder Kubota diesel engine connected to a Leroy Somer 8 kW brushless self-regulated generator as well as the PV array. The system operated in this mode until the VRB SOC was greater than the upper threshold SOC.

The Guggenberger et al. (2012) model predicted the microgrid performance according to equation (6),

$$P_{Out\ MPPT} + P_{VRB} + P_{DC\ Load} = h_{inverter}(P_{HVAC} + P_{AC\ Load} + P_{Generator}) \quad (6)$$

where $P_{Out\ MPPT}$ is the power available to the system after the maximum power point tracking (MPPT), P_{VRB} is the power charged or discharged from the VRB, $P_{DC\ Load}$ is the peak DC load available to the system, P_{HVAC} is the power used by the VRB's HVAC system, $P_{AC\ Load}$ is the peak AC load that is available to the system, $P_{Generator}$ is the power of the generator, and $h_{inverter}$ is the efficiency of the inverter.

Monte Carlo modeling of the microgrids at TA-246 and B2222 was performed using the Oracle ® Crystal Ball Version 11.1.275.0 spreadsheet-based application for Microsoft Excel.

1. *Method I.* GHI, ambient temperature, VRB SOC, and the energy load were all modeled as random variables. For these variables, PDFs were used to generate values based on a probability distribution fit to a data set for each trial the model runs. One initial VRB SOC was simulated for January 1st at 1 AM. This scenario modeled continuous operation of the microgrid from January through December.
2. *Method II.* This scenario was identical to Method I except that a unique VRB SOC was stochastically generated for the first hour of each month. This scenario modeled discontinuous operation of the microgrid on a monthly interval.
3. *Method III.* This scenario was identical to Method I except that it was assumed that the VRB was recharged at the beginning of each month, and the VRB SOC was set to 16kWh for TA-246 and 14.6kWh for B2222 for the first hour of each month.

A sensitivity analysis was performed on the number of Monte Carlo simulations, and the output ensemble of the diesel generator operation time was found to stabilize at 1,000 realizations.

4. RESULTS

The percent of time the generator was running the system is recorded for each month of the year. The average percent time the generator was running is calculated for each month and compared to the results of the other two methods. The results of all three methods are also compared to the deterministic model used in Guggenberger et al. (2012). Stochastic results for TA-246 show that the average annual operating times for

the generator in Methods I, II, and III were relatively close. The average percent of the generator running time was 14.96 percent for Method I, 15.08 percent for Method II, and 14.96 percent for Method III. These stochastic predictions agreed with the deterministic prediction of 14.8 percent for the year. Figure 4 shows that there are more significant differences at monthly intervals although the stochastic results were relatively similar. Differences in the modeling results from the deterministic results in the later months due to having partial energy load sets.

The performance results of microgrid B2222 were also compared to the deterministic modeling of the system. Methods I, II, and III all still showed performance results that were similar to one another, however, they did differ from the deterministic method. Method I, II, and III results for the months of June, July, and August were identical to the results of the deterministic model. For the year, the percent time generator running for Method I was 13.47 percent, Method II was 13.54 percent, and Method III was also 13.47 percent. The deterministic model time generator running averaged 13.70 percent for the year.

Altering the VRB SOC in three methods also shows that changing the way VRB SOC is treated in the model does have a slight effect on the predicted performance, but does not make a significant change. This is due to the VRB SOC only being altered for one hour at the beginning of each year/month with the following SOC's being calculated from equation (5). The VRB is also constantly being recharged throughout each day in order to keep the SOC within the upper and lower thresholds.

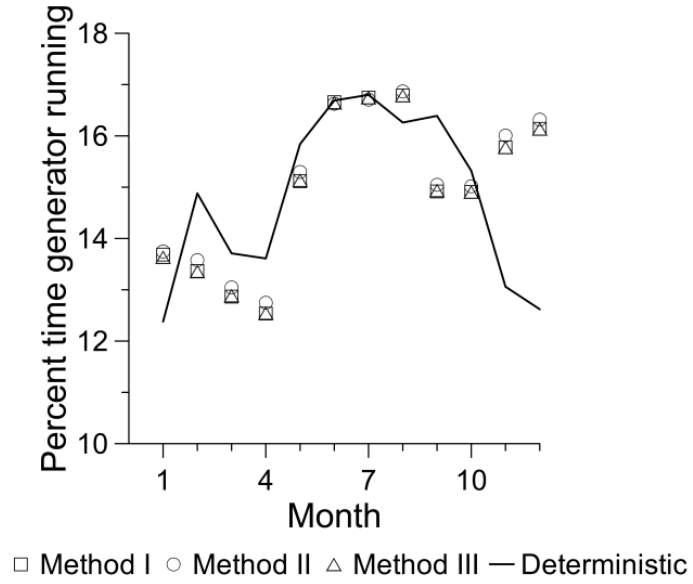


Fig. 4. TA-246 Modeling Results

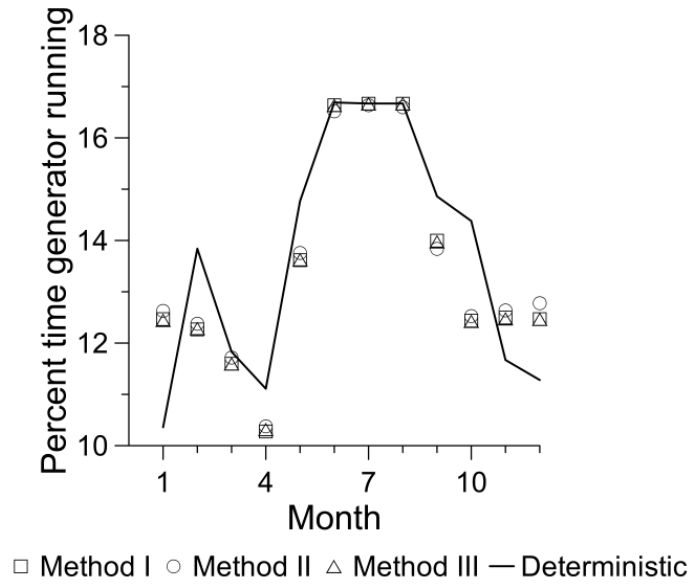


Fig. 5. B2222 Modeling Results

The model results of B2222 are also compared to real performance data collected from the B2222 site from May 2013. The observed number of hours that the system operated on the grid was compared to the simulated cumulative percent of the time the generator was running. For May 2013, B2222 operated on the grid for 102 hours. For Method I, the generator shows a 49 percent probability of running at least 102 hours or less. For Method II, the generator has a 38 percent probability or less of running for that amount of time or less, and for Method III, the generator has a 48 percent probability. All three values were in the central range of the cumulative probability range of the 25 to 75 percent. Additional months of performance data were not available to assess if the stochastic models would tend to over or under predict the use of the diesel generator. The deterministic results predicted that the system would run the diesel generator for a total of 107 hours for the month of May.

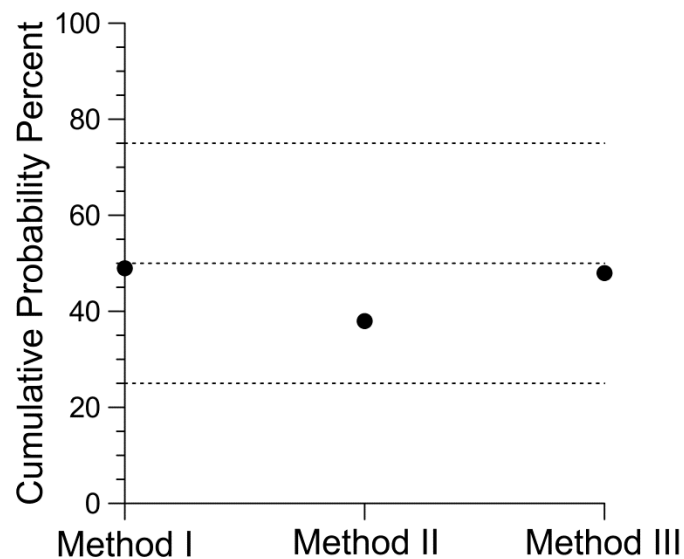


Fig. 6. Comparison of B2222 Modeling Results to Measured Performance

5. CONCLUSIONS

This study stochastically characterized GHI and ambient temperature using a TMY3 data set, VRB SOC was characterized using engineering judgment, and energy load were stochastically characterized using observed data. PDFs of the random variables were incorporated into a deterministic PV performance model in order to create a Monte Carlo based stochastic PV performance model. The analysis for three different initial SOC scenarios indicated that the stochastic analysis was relatively insensitive to the initial state of the battery. Finally, there were insufficient microgrid performance data available to conclusively characterize the reliability of the stochastic model. However, the available data indicated that the modeling techniques presented in this paper may have the potential for wider applicability given the nationwide availability of TMY3 data. The applicability could be expanded further by modifying the basic model to include other energy systems beyond VRBs.

NOTATION LIST

The following symbols are used in this paper:

H	Solar hour angle ($^{\circ}$);
I_B	Beam insolation (W/m^2);
I_{BC}	Beam insolation striking collector face (W/m^2);
I_{BN}	Beam insolation normal to the collector face (W/m^2);
L	Latitude ($^{\circ}$);
n	Ordinal day number
β	Solar altitude angle ($^{\circ}$);
δ	Declination angle ($^{\circ}$);
θ	Incidence angle between sun and collector face ($^{\circ}$); and
Σ	Collector tilt angle ($^{\circ}$).

REFERENCES

- Ang, A.H.S. and Tang, W.H. (1975). "Probability concepts in engineering planning and design volume I – basic principles." *John Wiley & Sons, Inc.*, New York, NY, 129-133.
- Arabali, A., Ghofrani, M., Etezadi-Amoli, M., and Fadali, M.S. (2014). "Stochastic performance assessment and sizing for a hybrid power systems of solar/wind/energy storage." *IEEE Trans. Sustainable Energy*, 5(2), 363-371.
- Bandara, K., Sweet, T., and Ekanayake, J. (2012). "Photovoltaic applications for off-grid electrification using novel multi-level inverter technology with energy storage." *Renewable Energy*, 37(2012), 82-88.
- Fossati, J.P., Galarza, A., Martin-Villate, A., and Fontan, L. (2015). "A method for optimal sizing energy storage systems for microgrids." *Renewable Energy*, 77(2015), 539-549.
- Guggenberger, J.D., Elmore, A.C., and Tichenor, J.L., Crow, M.L. (2012). "Performance prediction of a vanadium redox battery for use in portable, scalable microgrids." *IEEE Transactions on smart Grid*, 3(4), 2109-2116.
- Karaki, S.H., Chedid, R.B., and Ramadan, R. (1999). "Probabilistic performance assessment of autonomous solar-wind energy conversion systems." *IEEE Trans. on Energy Convers.*, 14(3), 766-772.
- Khatod, D.K., Pant, V., and Sharma, J. (2010). "Analytical approach for well-being assessment of small autonomous power systems with solar and wind energy sources." *IEEE Trans. Energy Convers.*, 25(2), 535-545.
- Kishore, L.N. and Fernandez, E. (2011). "Reliability well-being assessment of PV-wind hybrid system using Monte Carlo simulation." *Proc. Int. Conf. Emerging Trends in Electrical and Computer Technology (ICETECT)*, 63-68.
- Masters, G.M. (2013). "Renewable and efficient electrical power systems." *John Wiley & Sons, Inc.*, Hoboken, NJ.

Merei, G., Berger, C., and Sauer, D.U. (2013). "Optimization of an off-grid hybrid PV-wind-Diesel system with different battery technologies using genetic algorithm." *Solar Energy*, 97(2013), 460-473.

Nguyen, T.A., Xin Q., Guggenberger II, J.D, Crow, M.L., and Elmore, A.C. (2013). "Performance characterization for photovoltaic-vanadium redox battery microgrid systems." *IEEE Trans. on Sustainable Energy*, in press.

Patterson, M., Macia, N.F., and Kannan, A.M. (2014). "Hybrid microgrid model based on solar photovoltaic battery fuel cell system for intermittent load applications." *IEEE Trans. Energy Convers.*, in press.

Provata, E., Kolokotsa, D., Papantoniou, S., Pietrini, M., Giovannelli, A., and Romiti, G. (2015). "Development of optimization algorithms for the Leaf community microgrid." *Renewable Energy*, 74(2015), 782-795.

Salameh, Z.M., Borowy, B.S., and Amin, A.R.A. (1995). "Photovoltaic module-site matching based on capacity factors." *IEEE Transactions on Energy Convers.*, 10(2), 326-331.

Wilcox, S. and Marion, W. (2008). "User's manual for TMY3 data sets." *National Renewable Energy Laboratory (NREL)*, Golden, CO.

SECTION

4. RECOMMENDATIONS FOR FUTURE WORK

The following are suggestions for further development of the research presented in this paper.

- More detailed examination of the correlation between HVAC and ambient temperature
- Using a larger set of collected energy load data to better characterize the energy load when creating PDFs
- Improving the user interface, possibly with another program, of the model to allow for easier PDF parameter inputs
- Applying the model to a wider range microgrid sites throughout the United States
- Including other components to the model such as different energy storage systems or other types of renewable energy.

APPENDIX A.

PARAMETERS FOR STOCHASTIC VARIABLES

Month	Parameter	Hour											
		7	8	9	10	11	12	13	14	15	16	17	18
Jan	P				1.2	0.71	1.3	0.79	4.7	2.2			
	Q				1.0	0.31	1.6	1.2	11	2.3			
Feb	P				1.8	1.4	2.0	2.9	2.9	5.3			
	Q				1.9	1.0	1.5	2.8	2.2	4.8			
Mar	P			0.86	0.59	0.98	0.92	1.7	1.0	1.3			
	Q			1.4	0.46	1.5	1.9	3.3	1.6	2.3			
Apr	P		1.5	1.2	1.4	2.2	1.7	2.3	3.2	2.8	3.0	3.0	
	Q		2.5	1.3	1.4	2.5	1.5	1.9	3.4	2.2	3.3	2.8	
May	P		4.6	3.1	1.2	1.6	4.9	2.1	3.5	2.7	2.4	1.4	1.5
	Q		5.5	0.75	0.3	1.1	3.6	1.4	1.1	1.1	0.6	0.6	1.1
Jun	P	4.9	3.9	3.3	2.2	1.6	1.5	1.9	2.0	2.5	1.9	1.6	3.0
	Q	7.6	3.2	1.5	0.95	0.83	0.86	0.89	1.4	1.9	1.1	0.79	2.0
July	P		8.2	7.3	5.7	5.2	2.1	2.5	3.7	1.6	1.7	2.8	3.9
	Q		5.9	2.5	0.89	0.83	0.5	0.8	1.2	0.78	0.4	0.63	0.61
Aug	P		3.5	2.6	1.4	1.5	2.0	2.1	4.3	4.3	2.2	4.7	
	Q		4.8	1.8	0.53	0.59	1.4	1.3	2.0	2.4	0.87	1.4	
Sep	P			1.8	1.3	1.1	3.3	1.6	3.5	1.3	1.8	2.2	
	Q			1.2	0.65	0.86	3.9	1.2	3.7	0.92	1.2	1.8	
Oct	P			1.1	0.95	0.90	0.93	0.94	0.82	1.3	2.4		
	Q			0.85	0.50	0.54	0.66	0.52	0.54	1.0	1.1		
Nov	P				1.2	1.7	1.5	1.9	1.4	1.4	1.7		
	Q				1.6	2.4	1.9	2.6	1.5	1.5	1.8		
Dec	P				1.5	1.3	1.5	1.5	1.7	1.9	2.5		
	Q				1.8	1.1	1.4	1.4	1.5	1.6	1.9		

Table A.1. GHI beta distribution parameters

	TA-246	B2222
Maximum (kWh)	20	20
Upper Threshold (kWh)	16	14.6
Lower Threshold (kWh)	6	4

Table A.2. VRB SOC uniform distribution parameters

		Hour											
		1	2	3	4	5	6	7	8	9	10	11	12
Jan	Location	6.54	6.5	6.52	6.51	6.5	6.52	6.51	6.48	6.46	6.48	6.53	6.54
	Scale	0.146	0.112	0.114	0.111	0.141	0.173	0.104	0.101	0.121	0.094	0.204	0.185
Feb	Location	6.44	6.43	6.49	6.47	6.44	6.46	6.42	6.44	6.44	6.47	6.53	6.55
	Scale	0.12	0.166	0.113	0.148	0.116	0.168	0.129	0.171	0.146	0.16	0.174	0.179
Mar	Location	6.68	6.64	6.65	6.63	6.63	6.65	6.58	6.64	6.61	6.72	6.76	6.73
	Scale	0.152	0.173	0.189	0.147	0.134	0.157	0.149	0.14	0.196	0.171	0.175	0.168
Apr	Location	6.68	6.73	6.72	6.73	6.66	6.73	6.72	6.67	6.7	6.74	6.75	6.76
	Scale	0.182	0.195	0.189	0.168	0.2	0.17	0.174	0.156	0.223	0.22	0.201	0.152
May	Location	6.63	6.83	6.7	6.76	6.69	6.81	6.72	6.68	6.81	6.74	6.82	6.84
	Scale	0.206	0.169	0.223	0.199	0.23	0.155	0.174	0.179	0.194	0.25	0.208	0.175
Jun	Location	6.71	6.84	6.86	6.71	6.83	6.83	6.78	6.83	6.8	6.84	6.77	6.8
	Scale	0.198	0.162	0.217	0.192	0.224	0.137	0.166	0.223	0.182	0.207	0.207	0.193
Jul	Location	6.8	6.86	6.96	6.7	6.95	6.82	6.83	6.95	6.82	6.85	6.84	6.76
	Scale	0.132	0.103	0.102	0.155	0.125	0.148	0.128	0.122	0.15	0.197	0.212	0.201
Aug	Location	6.9	6.76	6.86	6.84	6.72	6.89	6.77	6.87	6.83	6.84	6.85	6.77
	Scale	0.205	0.224	0.219	0.215	0.218	0.14	0.193	0.191	0.198	0.17	0.216	0.261
Sep	Location	6.89	6.74	6.82	6.89	6.69	6.85	6.76	6.89	6.79	6.85	6.9	6.7
	Scale	0.184	0.189	0.284	0.208	0.143	0.155	0.182	0.109	0.142	0.183	0.239	0.257
Oct	Location	6.79	6.78	6.74	6.88	6.7	6.83	6.76	6.88	6.72	6.84	6.86	6.72
	Scale	0.184	0.189	0.284	0.208	0.143	0.155	0.182	0.109	0.142	0.183	0.239	0.257
Nov	Location	6.67	6.61	6.65	6.67	6.63	6.65	6.68	6.65	6.6	6.63	6.73	6.61
	Scale	0.166	0.154	0.199	0.216	0.132	0.14	0.219	0.215	0.174	0.221	0.269	0.209
Dec	Location	6.55	6.53	6.5	6.51	6.56	6.55	6.5	6.47	6.46	6.47	6.51	6.47
	Scale	0.146	0.112	0.114	0.111	0.141	0.173	0.104	0.101	0.121	0.094	0.204	0.185

Table A.3. Energy load lognormal distribution parameters

		Hour											
		13	14	15	16	17	18	19	20	21	22	23	24
Jan	Location	6.59	6.59	6.6	6.6	6.58	6.58	6.54	6.58	6.53	6.53	6.5	6.53
	Scale	0.151	0.137	0.166	0.165	0.137	0.158	0.217	0.171	0.139	0.13	0.152	0.15
Feb	Location	6.55	6.55	6.58	6.67	6.55	6.55	6.51	6.54	6.5	6.46	6.47	6.52
	Scale	0.117	0.16	0.134	0.13	0.163	0.142	0.151	0.135	0.168	0.144	0.145	0.124
Mar	Location	6.73	6.68	6.71	6.78	6.71	6.71	6.7	6.72	6.65	6.77	6.69	6.65
	Scale	0.111	0.096	0.099	0.131	0.172	0.159	0.158	0.152	0.14	0.121	0.133	0.121
Apr	Location	6.74	6.71	6.73	6.76	6.71	6.68	6.77	6.72	6.69	6.76	6.67	6.79
	Scale	0.193	0.203	0.176	0.188	0.209	0.199	0.166	0.166	0.151	0.166	0.155	0.163
May	Location	6.75	6.81	6.71	6.78	6.79	6.73	6.81	6.73	6.71	6.84	6.66	6.88
	Scale	0.23	0.246	0.258	0.242	0.242	0.244	0.189	0.188	0.166	0.145	0.184	0.187
Jun	Location	6.74	6.78	6.68	6.78	6.68	6.69	6.78	6.72	6.81	6.83	6.77	6.88
	Scale	0.16	0.188	0.226	0.184	0.254	0.253	0.154	0.166	0.15	0.105	0.175	0.162
Jul	Location	6.82	6.77	6.76	6.78	6.64	6.73	6.74	6.76	6.89	6.83	6.85	6.91
	Scale	0.109	0.187	0.251	0.12	0.233	0.233	0.143	0.179	0.133	0.143	0.168	0.136
Aug	Location	6.79	6.69	6.7	6.67	6.64	6.67	6.73	6.73	6.83	6.85	6.78	6.81
	Scale	0.206	0.261	0.246	0.237	0.238	0.242	0.229	0.198	0.193	0.215	0.222	0.2
Sep	Location	6.75	6.62	6.62	6.59	6.57	6.54	6.65	6.77	6.78	6.79	6.84	6.78
	Scale	0.201	0.272	0.217	0.193	0.177	0.156	0.186	0.101	0.126	0.165	0.133	0.134
Oct	Location	6.72	6.6	6.62	6.58	6.59	6.53	6.54	6.78	6.76	6.79	6.8	6.81
	Scale	0.201	0.272	0.217	0.193	0.177	0.156	0.186	0.101	0.126	0.165	0.133	0.134
Nov	Location	6.63	6.73	6.62	6.61	6.63	6.67	6.64	6.68	6.66	6.59	6.65	6.69
	Scale	0.191	0.152	0.186	0.159	0.131	0.157	0.182	0.187	0.142	0.157	0.197	0.185
Dec	Location	6.5	6.58	6.59	6.56	6.59	6.55	6.55	6.56	6.51	6.48	6.47	6.53
	Scale	0.151	0.137	0.166	0.165	0.137	0.158	0.217	0.171	0.139	0.13	0.152	0.15

Table A.4. Cont'd Energy load lognormal distribution parameters

Month	Catergory	Time Range	Location	Scale
January	Cooling AM	1:00-8:00	0.149	0.370
	Warming	9:00-16:00	0.573	1.48
	Cooling PM	17:00-0:00	0.482	1.22
February	Cooling AM	1:00-8:00	0.271	0.720
	Warming	9:00-16:00	0.968	2.52
	Cooling PM	17:00-0:00	0.739	1.91
March	Cooling AM	1:00-6:00	0.148	0.570
	Warming	7:00-16:00	0.498	1.36
	Cooling PM	17:00-0:00	0.441	1.10
April	Cooling AM	1:00-7:00	0.214	0.610
	Warming	8:00-16:00	0.956	2.39
	Cooling PM	17:00-0:00	1.01	2.56
May	Cooling AM	1:00-6:00	0.500	1.03
	Warming	7:00-16:00	1.33	3.31
	Cooling PM	17:00-0:00	1.17	2.92
June	Cooling AM	1:00-6:00	0.387	0.810
	Warming	7:00-16:00	1.04	2.61
	Cooling PM	17:00-0:00	0.907	2.27
July	Cooling AM	1:00-6:00	0.529	1.06
	Warming	7:00-16:00	1.34	3.35
	Cooling PM	17:00-0:00	1.08	2.68
August	Cooling AM	1:00-7:00	0.250	0.900
	Warming	8:00-16:00	0.941	2.36
	Cooling PM	17:00-0:00	0.941	2.38
September	Cooling AM	1:00-7:00	0.339	0.840
	Warming	8:00-16:00	1.05	2.65
	Cooling PM	17:00-0:00	0.847	2.13
October	Cooling AM	1:00-7:00	0.214	0.520
	Warming	8:00-16:00	1.16	2.96
	Cooling PM	17:00-0:00	1.05	2.67
November	Cooling AM	1:00-8:00	0.195	0.530
	Warming	9:00-16:00	0.466	1.21
	Cooling PM	17:00-0:00	0.323	0.810
December	Cooling AM	1:00-8:00	0.194	0.490
	Warming	9:00-16:00	0.558	1.50
	Cooling PM	17:00-0:00	0.411	1.03

Table A.5. Ambient Temperature parameters

APPENDIX B.

PROBABILITY AND DISTRIBUTION FITS

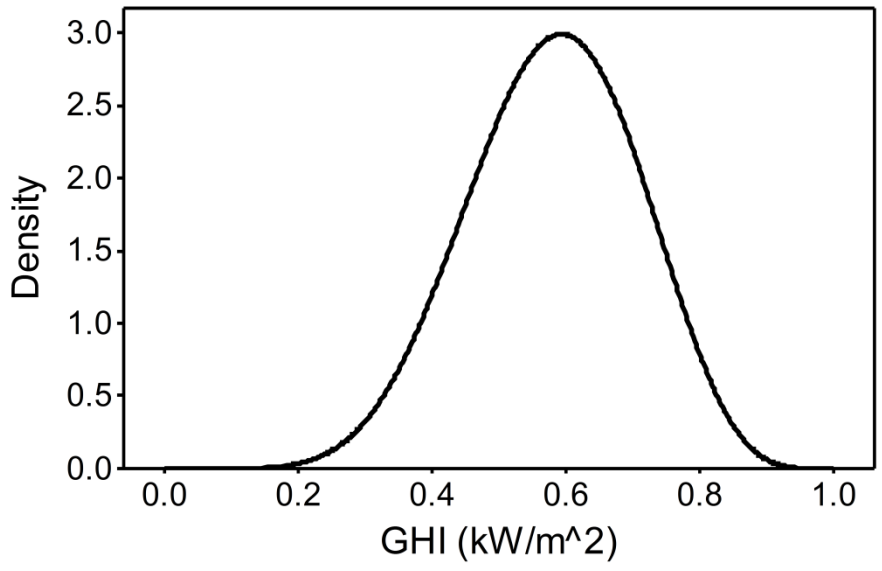


Figure B.1. GHI PDF for July 8AM

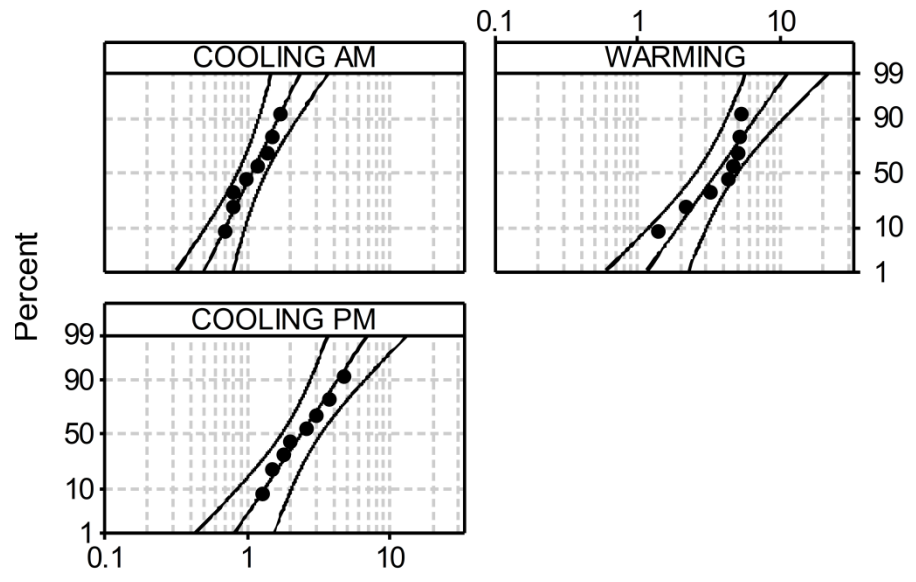


Figure B.2. Ambient Temperature Probability Fits for January

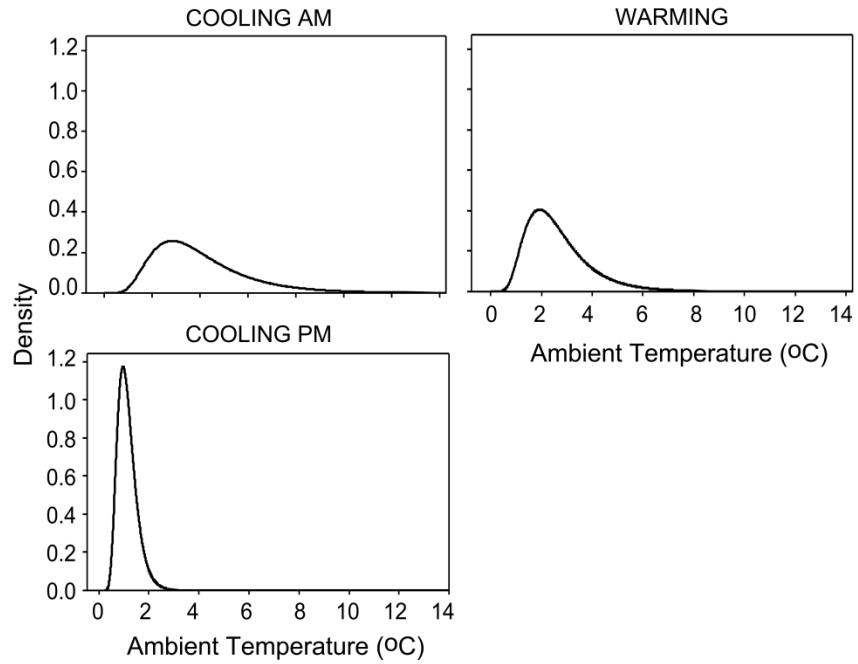


Figure B.3. Ambient Temperature PDFs for January

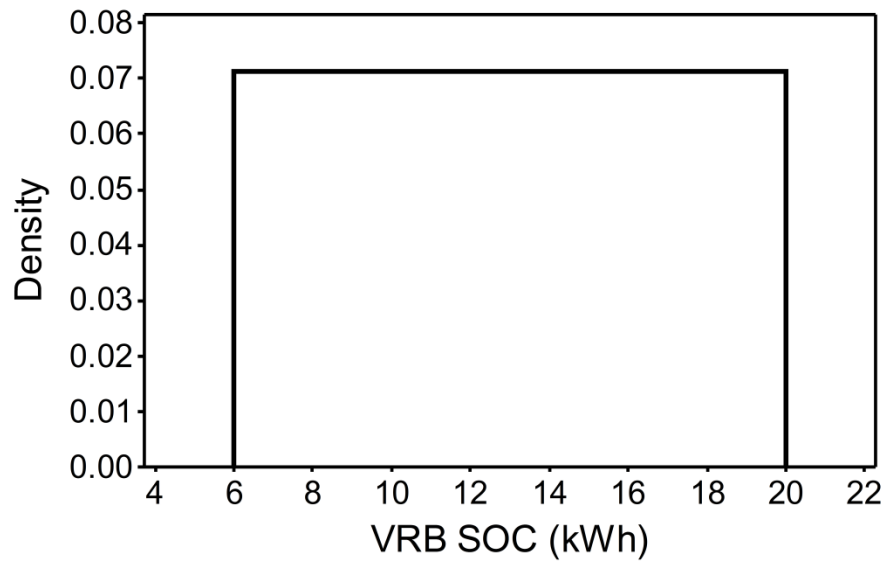


Figure B.4. VRB SOC PDF for Microgrid TA-246

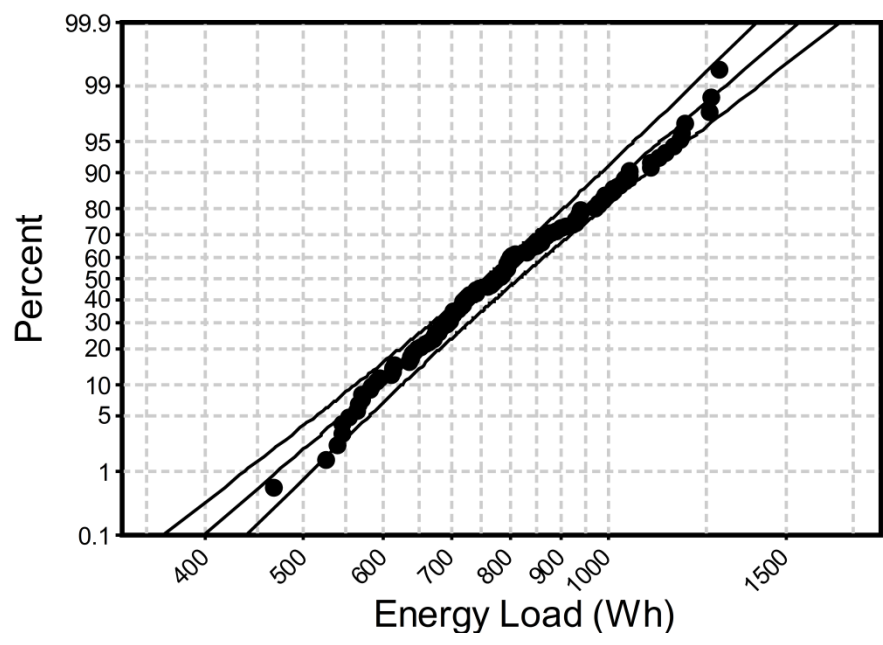


Figure B.5. Energy Load Probability Fit for 8AM January

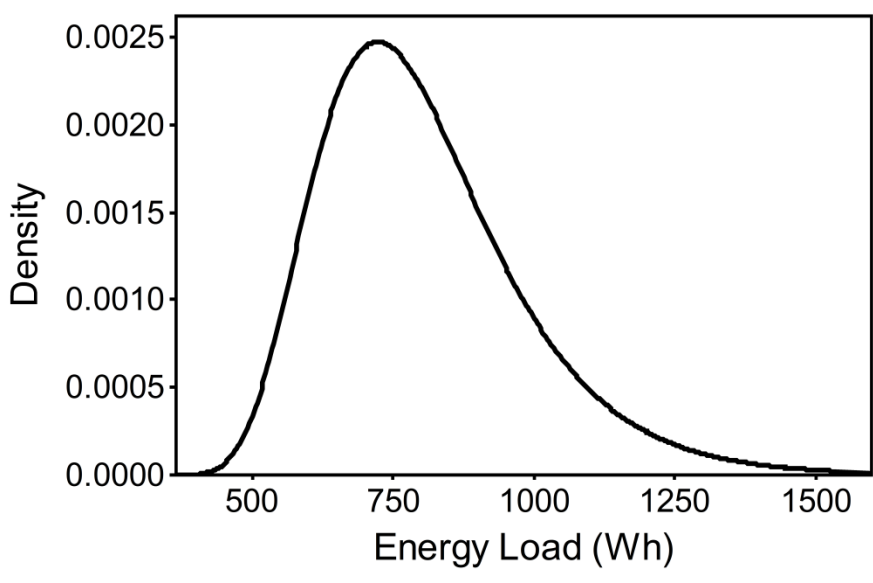


Figure B.6. Energy Load PDF for 8AM January

APPENDIX C.

CORRELATION TABLES

Hour	1	2	3	4	5	6	7	8	9	10	11	12	13	14	15	16	17	18	19	20	21	22	23	
2	0.998																							
3	0.993	0.998																						
4	0.985	0.993	0.998																					
5	0.974	0.985	0.994	0.998																				
6	0.960	0.975	0.986	0.994	0.999																			
7	0.955	0.971	0.983	0.991	0.996	0.998																		
8	0.941	0.958	0.972	0.983	0.990	0.994	0.997																	
9	0.908	0.929	0.946	0.960	0.970	0.977	0.982	0.991																
10	0.864	0.887	0.908	0.924	0.938	0.948	0.954	0.969	0.991															
11	0.808	0.832	0.854	0.871	0.885	0.897	0.906	0.928	0.967	0.987														
12	0.756	0.782	0.805	0.824	0.840	0.853	0.864	0.891	0.938	0.969	0.992													
13	0.696	0.723	0.748	0.770	0.788	0.803	0.815	0.845	0.898	0.935	0.963	0.981												
14	0.662	0.690	0.716	0.740	0.759	0.776	0.789	0.820	0.877	0.915	0.949	0.968	0.996											
15	0.640	0.669	0.695	0.719	0.738	0.756	0.769	0.801	0.860	0.900	0.937	0.959	0.991	0.998										
16	0.635	0.664	0.691	0.714	0.735	0.752	0.766	0.799	0.859	0.899	0.938	0.960	0.988	0.996	0.998									
17	0.648	0.677	0.703	0.727	0.747	0.764	0.778	0.809	0.866	0.903	0.936	0.956	0.986	0.994	0.996	0.997								
18	0.710	0.736	0.759	0.779	0.796	0.810	0.823	0.851	0.899	0.927	0.947	0.961	0.986	0.987	0.986	0.983	0.989							
19	0.731	0.755	0.776	0.794	0.809	0.821	0.835	0.862	0.901	0.918	0.930	0.935	0.965	0.966	0.963	0.958	0.969	0.990						
20	0.752	0.774	0.793	0.809	0.821	0.831	0.842	0.865	0.902	0.917	0.920	0.926	0.952	0.948	0.945	0.938	0.954	0.981	0.990					
21	0.746	0.766	0.783	0.797	0.808	0.817	0.830	0.853	0.890	0.905	0.911	0.919	0.941	0.938	0.934	0.930	0.945	0.971	0.980	0.994				
22	0.747	0.767	0.784	0.798	0.810	0.818	0.830	0.852	0.888	0.903	0.907	0.914	0.937	0.935	0.931	0.929	0.943	0.969	0.978	0.990	0.998			
23	0.744	0.764	0.780	0.794	0.805	0.813	0.825	0.846	0.880	0.894	0.897	0.904	0.926	0.925	0.923	0.923	0.935	0.961	0.970	0.981	0.990	0.997		
24	0.737	0.757	0.773	0.787	0.798	0.805	0.815	0.836	0.869	0.882	0.884	0.891	0.913	0.913	0.910	0.913	0.924	0.949	0.958	0.967	0.977	0.990	0.997	

Table C.1. January Hourly Ambient Temperature Correlations

Hour	1	2	3	4	5	6	7	8	9	10	11	12	13	14	15	16	17	18	19	20	21	22	23		
2	0.999																								
3	0.996	0.999																							
4	0.990	0.996	0.999																						
5	0.986	0.992	0.997	0.999																					
6	0.980	0.988	0.994	0.997	0.999																				
7	0.976	0.985	0.991	0.995	0.997	0.998																			
8	0.970	0.979	0.986	0.991	0.994	0.996	0.995																		
9	0.957	0.965	0.972	0.976	0.978	0.979	0.978	0.988																	
10	0.934	0.944	0.952	0.958	0.961	0.963	0.963	0.975	0.994																
11	0.915	0.924	0.933	0.939	0.942	0.944	0.943	0.956	0.982	0.993															
12	0.892	0.903	0.911	0.918	0.921	0.923	0.922	0.936	0.966	0.983	0.995														
13	0.868	0.878	0.887	0.894	0.896	0.898	0.900	0.911	0.943	0.963	0.979	0.990													
14	0.837	0.847	0.855	0.861	0.863	0.864	0.867	0.878	0.909	0.931	0.951	0.970	0.992												
15	0.826	0.836	0.844	0.850	0.852	0.853	0.856	0.867	0.898	0.920	0.943	0.964	0.987	0.997											
16	0.841	0.851	0.859	0.866	0.868	0.870	0.872	0.881	0.911	0.930	0.955	0.972	0.987	0.991	0.996										
17	0.837	0.848	0.858	0.866	0.870	0.873	0.873	0.884	0.904	0.922	0.944	0.960	0.971	0.975	0.980	0.989									
18	0.815	0.827	0.837	0.846	0.850	0.854	0.855	0.866	0.892	0.911	0.935	0.953	0.969	0.976	0.982	0.988	0.992								
19	0.804	0.816	0.827	0.835	0.840	0.843	0.847	0.857	0.885	0.904	0.930	0.947	0.966	0.974	0.979	0.984	0.988	0.997							
20	0.787	0.798	0.806	0.814	0.817	0.820	0.825	0.835	0.868	0.890	0.918	0.939	0.962	0.973	0.980	0.982	0.983	0.995	0.996						
21	0.783	0.794	0.804	0.811	0.816	0.819	0.823	0.834	0.866	0.888	0.915	0.935	0.955	0.964	0.970	0.974	0.980	0.993	0.996	0.997					
22	0.773	0.784	0.794	0.801	0.806	0.809	0.813	0.823	0.855	0.877	0.906	0.927	0.948	0.959	0.966	0.971	0.979	0.992	0.994	0.996	0.999				
23	0.760	0.772	0.782	0.790	0.794	0.798	0.801	0.811	0.842	0.865	0.896	0.918	0.939	0.951	0.960	0.966	0.976	0.989	0.991	0.994	0.997	0.999			
24	0.747	0.758	0.768	0.776	0.780	0.784	0.787	0.797	0.827	0.851	0.884	0.906	0.929	0.942	0.953	0.960	0.971	0.984	0.986	0.989	0.992	0.997	0.999		

Table C.2. February Hourly Ambient Temperature Correlations

Hour	1	2	3	4	5	6	7	8	9	10	11	12	13	14	15	16	17	18	19	20	21	22	23
2	0.999																						
3	0.997	0.999																					
4	0.993	0.997	0.999																				
5	0.987	0.993	0.997	0.999																			
6	0.980	0.987	0.993	0.997	0.999																		
7	0.978	0.984	0.990	0.994	0.996	0.997																	
8	0.971	0.977	0.982	0.985	0.987	0.987	0.991																
9	0.955	0.960	0.964	0.966	0.967	0.966	0.972	0.989															
10	0.936	0.941	0.946	0.948	0.949	0.948	0.956	0.979	0.993														
11	0.916	0.920	0.924	0.925	0.925	0.923	0.933	0.961	0.980	0.991													
12	0.897	0.902	0.906	0.908	0.909	0.909	0.923	0.951	0.970	0.986	0.995												
13	0.872	0.877	0.882	0.884	0.885	0.885	0.901	0.934	0.956	0.975	0.990	0.996											
14	0.849	0.855	0.859	0.862	0.864	0.865	0.882	0.916	0.942	0.962	0.980	0.990	0.995										
15	0.846	0.851	0.854	0.856	0.856	0.856	0.873	0.906	0.932	0.950	0.970	0.981	0.986	0.995									
16	0.797	0.801	0.803	0.805	0.805	0.805	0.824	0.857	0.888	0.909	0.931	0.947	0.954	0.971	0.981								
17	0.793	0.797	0.800	0.802	0.803	0.803	0.823	0.855	0.885	0.907	0.929	0.945	0.952	0.969	0.979	0.999							
18	0.792	0.797	0.801	0.804	0.805	0.806	0.825	0.859	0.891	0.914	0.937	0.950	0.959	0.974	0.980	0.995	0.998						
19	0.802	0.807	0.811	0.814	0.816	0.817	0.836	0.871	0.901	0.918	0.940	0.953	0.958	0.970	0.973	0.987	0.989	0.992					
20	0.802	0.808	0.813	0.816	0.818	0.819	0.838	0.874	0.903	0.922	0.945	0.956	0.963	0.972	0.973	0.983	0.986	0.991	0.998				
21	0.824	0.829	0.834	0.838	0.840	0.841	0.857	0.892	0.919	0.935	0.955	0.960	0.966	0.972	0.972	0.972	0.976	0.985	0.991	0.995			
22	0.823	0.829	0.834	0.837	0.839	0.840	0.856	0.892	0.918	0.934	0.953	0.958	0.965	0.970	0.969	0.967	0.972	0.982	0.989	0.993	0.999		
23	0.821	0.826	0.831	0.835	0.836	0.838	0.854	0.889	0.914	0.931	0.950	0.954	0.961	0.966	0.964	0.961	0.966	0.978	0.984	0.989	0.997	0.999	
24	0.818	0.823	0.828	0.832	0.834	0.835	0.851	0.886	0.911	0.928	0.946	0.949	0.957	0.961	0.958	0.954	0.960	0.972	0.979	0.984	0.994	0.997	0.999

Table C.3. March Hourly Ambient Temperature Correlations

Hour	1	2	3	4	5	6	7	8	9	10	11	12	13	14	15	16	17	18	19	20	21	22	23
2	0.999																						
3	0.995	0.999																					
4	0.988	0.995	0.999																				
5	0.981	0.990	0.995	0.999																			
6	0.968	0.976	0.980	0.982	0.983																		
7	0.944	0.949	0.951	0.951	0.950	0.977																	
8	0.883	0.885	0.885	0.882	0.879	0.904	0.963																
9	0.767	0.768	0.765	0.762	0.758	0.777	0.858	0.924															
10	0.658	0.656	0.652	0.647	0.640	0.673	0.772	0.859	0.958														
11	0.575	0.570	0.564	0.557	0.549	0.581	0.687	0.777	0.921	0.953													
12	0.559	0.557	0.554	0.550	0.543	0.565	0.664	0.751	0.892	0.928	0.976												
13	0.577	0.581	0.581	0.582	0.578	0.593	0.681	0.754	0.885	0.916	0.944	0.975											
14	0.549	0.556	0.560	0.564	0.564	0.562	0.642	0.720	0.846	0.863	0.882	0.930	0.978										
15	0.551	0.557	0.559	0.563	0.563	0.553	0.628	0.701	0.821	0.823	0.852	0.904	0.959	0.989									
16	0.496	0.502	0.504	0.508	0.508	0.496	0.564	0.631	0.745	0.757	0.785	0.849	0.919	0.963	0.982								
17	0.382	0.385	0.386	0.389	0.387	0.383	0.467	0.548	0.700	0.738	0.770	0.823	0.886	0.936	0.943	0.966							
18	0.371	0.372	0.371	0.371	0.367	0.363	0.446	0.535	0.686	0.737	0.780	0.835	0.879	0.924	0.923	0.942	0.986						
19	0.362	0.362	0.360	0.359	0.356	0.368	0.457	0.530	0.656	0.696	0.753	0.799	0.840	0.874	0.883	0.908	0.959	0.976					
20	0.397	0.397	0.394	0.393	0.389	0.404	0.482	0.541	0.654	0.690	0.734	0.785	0.839	0.874	0.886	0.919	0.955	0.964	0.987				
21	0.448	0.449	0.448	0.447	0.443	0.456	0.520	0.568	0.662	0.694	0.731	0.774	0.838	0.875	0.887	0.920	0.949	0.954	0.972	0.989			
22	0.466	0.466	0.464	0.463	0.458	0.473	0.537	0.584	0.677	0.706	0.750	0.784	0.845	0.874	0.887	0.916	0.938	0.944	0.967	0.985	0.998		
23	0.482	0.481	0.479	0.477	0.472	0.488	0.552	0.599	0.689	0.714	0.764	0.790	0.847	0.868	0.883	0.907	0.921	0.929	0.957	0.975	0.990	0.998	
24	0.495	0.494	0.492	0.489	0.483	0.500	0.564	0.610	0.698	0.718	0.775	0.793	0.845	0.859	0.876	0.895	0.902	0.911	0.943	0.960	0.978	0.990	0.998

Table C.4. April Hourly Ambient Temperature Correlations

Hour	1	2	3	4	5	6	7	8	9	10	11	12	13	14	15	16	17	18	19	20	21	22	23
2	0.997																						
3	0.987	0.997																					
4	0.971	0.988	0.997																				
5	0.956	0.977	0.991	0.998																			
6	0.953	0.968	0.976	0.979	0.977																		
7	0.913	0.921	0.923	0.919	0.913	0.940																	
8	0.871	0.869	0.864	0.852	0.841	0.871	0.951																
9	0.810	0.804	0.794	0.778	0.765	0.808	0.914	0.977															
10	0.800	0.792	0.780	0.763	0.749	0.810	0.883	0.950	0.980														
11	0.791	0.782	0.770	0.753	0.740	0.801	0.873	0.942	0.968	0.984													
12	0.789	0.776	0.759	0.738	0.722	0.772	0.829	0.914	0.942	0.961	0.975												
13	0.805	0.792	0.775	0.754	0.738	0.794	0.851	0.922	0.942	0.961	0.978	0.983											
14	0.815	0.805	0.790	0.772	0.757	0.806	0.848	0.905	0.920	0.932	0.958	0.974	0.983										
15	0.817	0.805	0.790	0.770	0.755	0.809	0.862	0.918	0.927	0.939	0.955	0.969	0.984	0.986									
16	0.826	0.811	0.792	0.770	0.752	0.805	0.857	0.901	0.906	0.924	0.944	0.951	0.974	0.973	0.988								
17	0.811	0.797	0.780	0.757	0.741	0.806	0.862	0.891	0.900	0.922	0.920	0.911	0.948	0.931	0.962	0.977							
18	0.758	0.737	0.714	0.686	0.664	0.737	0.777	0.816	0.832	0.860	0.845	0.847	0.887	0.871	0.897	0.922	0.957						
19	0.707	0.688	0.666	0.640	0.621	0.696	0.771	0.833	0.854	0.884	0.872	0.876	0.902	0.872	0.893	0.905	0.933	0.966					
20	0.705	0.686	0.665	0.640	0.620	0.694	0.787	0.842	0.864	0.881	0.876	0.870	0.904	0.885	0.893	0.900	0.914	0.938	0.971				
21	0.715	0.696	0.674	0.648	0.629	0.701	0.791	0.843	0.865	0.881	0.879	0.877	0.908	0.893	0.901	0.905	0.916	0.937	0.971	0.998			
22	0.724	0.705	0.683	0.658	0.638	0.708	0.794	0.843	0.866	0.880	0.880	0.880	0.910	0.895	0.904	0.903	0.912	0.931	0.965	0.993	0.998		
23	0.729	0.710	0.688	0.663	0.643	0.710	0.792	0.838	0.862	0.873	0.876	0.878	0.906	0.892	0.901	0.896	0.903	0.921	0.955	0.983	0.991	0.998	
24	0.732	0.713	0.691	0.666	0.646	0.710	0.787	0.830	0.855	0.864	0.869	0.873	0.900	0.887	0.896	0.887	0.892	0.908	0.941	0.969	0.981	0.992	0.998

Table C.5. May Hourly Ambient Temperature Correlations

Hour	1	2	3	4	5	6	7	8	9	10	11	12	13	14	15	16	17	18	19	20	21	22	23	
2	0.995																							
3	0.981	0.996																						
4	0.960	0.983	0.996																					
5	0.939	0.969	0.987	0.997																				
6	0.906	0.928	0.946	0.950	0.950																			
7	0.818	0.837	0.858	0.863	0.867	0.945																		
8	0.768	0.781	0.795	0.794	0.795	0.878	0.881																	
9	0.679	0.687	0.702	0.698	0.698	0.788	0.808	0.945																
10	0.508	0.522	0.547	0.554	0.564	0.657	0.719	0.857	0.916															
11	0.452	0.465	0.490	0.497	0.508	0.604	0.675	0.829	0.902	0.985														
12	0.502	0.517	0.543	0.550	0.560	0.643	0.710	0.820	0.896	0.966	0.960													
13	0.545	0.566	0.595	0.606	0.619	0.682	0.741	0.832	0.880	0.897	0.898	0.952												
14	0.497	0.482	0.478	0.455	0.462	0.492	0.507	0.602	0.644	0.579	0.580	0.663	0.731											
15	0.454	0.438	0.430	0.407	0.413	0.431	0.459	0.546	0.593	0.539	0.548	0.625	0.700	0.984										
16	0.441	0.426	0.419	0.397	0.404	0.407	0.431	0.517	0.550	0.495	0.505	0.586	0.666	0.964	0.988									
17	0.470	0.457	0.453	0.433	0.440	0.437	0.451	0.538	0.577	0.514	0.529	0.610	0.683	0.970	0.972	0.979								
18	0.475	0.467	0.467	0.451	0.461	0.477	0.510	0.573	0.606	0.571	0.578	0.648	0.699	0.939	0.932	0.928	0.961							
19	0.483	0.471	0.465	0.446	0.454	0.475	0.490	0.577	0.581	0.525	0.530	0.597	0.645	0.929	0.917	0.899	0.920	0.955						
20	0.495	0.491	0.489	0.476	0.486	0.501	0.497	0.545	0.509	0.447	0.452	0.534	0.610	0.880	0.858	0.840	0.870	0.914	0.969					
21	0.501	0.497	0.494	0.481	0.490	0.507	0.503	0.548	0.513	0.455	0.458	0.538	0.603	0.865	0.842	0.824	0.856	0.909	0.968	0.997				
22	0.499	0.495	0.492	0.478	0.486	0.502	0.497	0.537	0.503	0.446	0.448	0.528	0.584	0.844	0.823	0.807	0.839	0.899	0.961	0.990	0.997			
23	0.494	0.491	0.488	0.476	0.483	0.500	0.498	0.533	0.500	0.448	0.448	0.527	0.573	0.817	0.795	0.781	0.813	0.883	0.949	0.977	0.989	0.997		
24	0.484	0.480	0.476	0.463	0.469	0.487	0.483	0.514	0.482	0.434	0.431	0.509	0.544	0.782	0.761	0.749	0.781	0.861	0.930	0.958	0.975	0.989	0.997	

Table C.6. June Hourly Ambient Temperature Correlations

Hour	1	2	3	4	5	6	7	8	9	10	11	12	13	14	15	16	17	18	19	20	21	22	23		
2	0.998																								
3	0.991	0.998																							
4	0.979	0.990	0.997																						
5	0.963	0.979	0.991	0.998																					
6	0.932	0.950	0.962	0.971	0.976																				
7	0.859	0.871	0.878	0.879	0.880	0.930																			
8	0.735	0.733	0.728	0.716	0.707	0.774	0.920																		
9	0.588	0.576	0.566	0.546	0.531	0.587	0.782	0.924																	
10	0.533	0.526	0.517	0.500	0.489	0.550	0.758	0.905	0.959																
11	0.500	0.496	0.489	0.477	0.469	0.531	0.732	0.871	0.927	0.975															
12	0.539	0.532	0.523	0.509	0.498	0.549	0.739	0.863	0.917	0.958	0.975														
13	0.435	0.432	0.426	0.416	0.410	0.459	0.661	0.782	0.849	0.903	0.950	0.946													
14	0.462	0.460	0.457	0.449	0.444	0.475	0.647	0.733	0.803	0.867	0.918	0.931	0.972												
15	0.408	0.410	0.410	0.406	0.404	0.427	0.592	0.646	0.717	0.788	0.860	0.867	0.920	0.967											
16	0.331	0.339	0.344	0.347	0.351	0.359	0.500	0.512	0.581	0.660	0.742	0.752	0.830	0.909	0.968										
17	0.349	0.350	0.347	0.343	0.340	0.352	0.486	0.505	0.570	0.644	0.703	0.712	0.788	0.863	0.928	0.958									
18	0.317	0.319	0.317	0.314	0.311	0.311	0.422	0.431	0.493	0.591	0.662	0.657	0.746	0.845	0.900	0.941	0.955								
19	0.334	0.334	0.329	0.324	0.318	0.313	0.444	0.467	0.532	0.626	0.700	0.705	0.791	0.870	0.906	0.928	0.933	0.972							
20	0.398	0.399	0.396	0.391	0.385	0.372	0.500	0.504	0.566	0.647	0.704	0.718	0.792	0.868	0.891	0.911	0.925	0.950	0.986						
21	0.420	0.421	0.419	0.414	0.409	0.397	0.522	0.526	0.582	0.662	0.721	0.733	0.808	0.880	0.900	0.914	0.925	0.948	0.985	0.998					
22	0.440	0.442	0.440	0.436	0.432	0.420	0.543	0.548	0.598	0.676	0.737	0.746	0.822	0.889	0.905	0.914	0.923	0.941	0.979	0.993	0.998				
23	0.469	0.473	0.471	0.469	0.465	0.453	0.572	0.577	0.620	0.693	0.755	0.759	0.833	0.895	0.906	0.908	0.914	0.929	0.968	0.982	0.991	0.997			
24	0.488	0.493	0.492	0.490	0.487	0.476	0.591	0.597	0.633	0.702	0.766	0.766	0.841	0.897	0.903	0.899	0.903	0.913	0.951	0.966	0.979	0.990	0.997		

Table C.7. July Hourly Ambient Temperature Correlations

Hour	1	2	3	4	5	6	7	8	9	10	11	12	13	14	15	16	17	18	19	20	21	22	23
2	0.996																						
3	0.984	0.996																					
4	0.964	0.984	0.996																				
5	0.947	0.972	0.989	0.998																			
6	0.934	0.959	0.976	0.985	0.988																		
7	0.936	0.945	0.945	0.937	0.927	0.927																	
8	0.762	0.765	0.757	0.744	0.729	0.735	0.882																
9	0.610	0.617	0.613	0.603	0.594	0.612	0.757	0.913															
10	0.492	0.501	0.499	0.492	0.485	0.497	0.618	0.787	0.920														
11	0.443	0.454	0.453	0.450	0.444	0.455	0.556	0.737	0.871	0.961													
12	0.423	0.431	0.425	0.418	0.409	0.414	0.504	0.673	0.821	0.911	0.964												
13	0.444	0.450	0.443	0.435	0.426	0.416	0.531	0.713	0.797	0.866	0.908	0.906											
14	0.462	0.464	0.454	0.443	0.428	0.409	0.513	0.683	0.718	0.767	0.795	0.806	0.950										
15	0.436	0.418	0.392	0.362	0.330	0.331	0.479	0.669	0.704	0.743	0.737	0.717	0.820	0.841									
16	0.397	0.375	0.349	0.319	0.287	0.275	0.461	0.655	0.675	0.701	0.681	0.648	0.749	0.751	0.945								
17	0.328	0.313	0.296	0.272	0.246	0.233	0.427	0.633	0.726	0.758	0.722	0.681	0.755	0.731	0.915	0.950							
18	0.345	0.329	0.311	0.285	0.260	0.250	0.452	0.652	0.765	0.771	0.726	0.689	0.738	0.699	0.878	0.915	0.977						
19	0.385	0.370	0.350	0.324	0.302	0.318	0.498	0.673	0.784	0.813	0.775	0.758	0.770	0.730	0.853	0.864	0.915	0.944					
20	0.489	0.477	0.460	0.435	0.415	0.425	0.569	0.693	0.788	0.814	0.768	0.751	0.754	0.728	0.830	0.822	0.871	0.902	0.974				
21	0.494	0.483	0.467	0.442	0.425	0.438	0.576	0.688	0.783	0.805	0.758	0.741	0.742	0.721	0.809	0.798	0.845	0.877	0.963	0.996			
22	0.508	0.500	0.487	0.465	0.450	0.466	0.595	0.694	0.780	0.793	0.745	0.730	0.732	0.715	0.785	0.773	0.812	0.845	0.943	0.984	0.995		
23	0.514	0.508	0.498	0.478	0.467	0.486	0.607	0.690	0.764	0.761	0.714	0.697	0.704	0.690	0.745	0.734	0.765	0.802	0.910	0.960	0.979	0.994	
24	0.515	0.511	0.504	0.487	0.479	0.501	0.609	0.677	0.742	0.728	0.682	0.666	0.674	0.664	0.703	0.689	0.713	0.752	0.870	0.928	0.954	0.978	0.995

Table C.8. August Hourly Ambient Temperature Correlations

Hour	1	2	3	4	5	6	7	8	9	10	11	12	13	14	15	16	17	18	19	20	21	22	23
2	0.998																						
3	0.992	0.998																					
4	0.983	0.992	0.998																				
5	0.973	0.985	0.994	0.998																			
6	0.972	0.983	0.992	0.996	0.998																		
7	0.970	0.979	0.984	0.985	0.983	0.985																	
8	0.954	0.954	0.951	0.945	0.935	0.936	0.962																
9	0.909	0.900	0.889	0.875	0.857	0.854	0.901	0.972															
10	0.860	0.847	0.830	0.812	0.789	0.786	0.836	0.923	0.978														
11	0.832	0.819	0.802	0.784	0.761	0.758	0.805	0.902	0.960	0.986													
12	0.758	0.744	0.725	0.707	0.682	0.681	0.739	0.850	0.924	0.948	0.978												
13	0.732	0.717	0.698	0.679	0.655	0.655	0.709	0.820	0.896	0.924	0.961	0.985											
14	0.701	0.687	0.671	0.654	0.631	0.632	0.689	0.802	0.877	0.904	0.946	0.976	0.994										
15	0.697	0.683	0.667	0.650	0.627	0.628	0.690	0.806	0.880	0.908	0.946	0.975	0.990	0.996									
16	0.704	0.692	0.675	0.659	0.637	0.636	0.697	0.813	0.887	0.916	0.948	0.972	0.986	0.993	0.997								
17	0.698	0.687	0.672	0.657	0.636	0.634	0.700	0.811	0.886	0.916	0.945	0.965	0.978	0.987	0.994	0.996							
18	0.751	0.743	0.731	0.717	0.697	0.699	0.762	0.855	0.909	0.923	0.947	0.960	0.968	0.975	0.982	0.982	0.987						
19	0.777	0.768	0.755	0.741	0.721	0.722	0.778	0.869	0.927	0.943	0.956	0.961	0.962	0.964	0.969	0.972	0.977	0.989					
20	0.760	0.751	0.739	0.726	0.707	0.710	0.765	0.855	0.909	0.925	0.939	0.938	0.941	0.950	0.957	0.961	0.967	0.982	0.992				
21	0.765	0.755	0.742	0.728	0.708	0.710	0.767	0.857	0.911	0.926	0.938	0.934	0.936	0.944	0.952	0.957	0.963	0.978	0.991	0.998			
22	0.771	0.761	0.747	0.732	0.711	0.714	0.770	0.859	0.915	0.928	0.938	0.932	0.933	0.939	0.947	0.952	0.958	0.973	0.988	0.993	0.999		
23	0.774	0.762	0.747	0.731	0.710	0.712	0.769	0.858	0.914	0.926	0.935	0.926	0.925	0.930	0.939	0.944	0.950	0.964	0.981	0.986	0.994	0.998	
24	0.776	0.764	0.748	0.731	0.710	0.711	0.768	0.856	0.912	0.922	0.929	0.917	0.915	0.918	0.927	0.932	0.938	0.952	0.972	0.975	0.987	0.994	0.998

Table C.9. September Hourly Ambient Temperature Correlations

Hour	1	2	3	4	5	6	7	8	9	10	11	12	13	14	15	16	17	18	19	20	21	22	23
2	0.999																						
3	0.997	0.999																					
4	0.993	0.997	0.999																				
5	0.990	0.994	0.998	1.000																			
6	0.987	0.991	0.994	0.996	0.996																		
7	0.981	0.983	0.984	0.984	0.983	0.991																	
8	0.942	0.940	0.936	0.932	0.927	0.935	0.959																
9	0.832	0.823	0.813	0.804	0.794	0.797	0.836	0.939															
10	0.798	0.792	0.784	0.776	0.769	0.769	0.800	0.919	0.970														
11	0.756	0.749	0.740	0.731	0.723	0.720	0.753	0.887	0.956	0.987													
12	0.682	0.675	0.667	0.657	0.649	0.649	0.684	0.824	0.909	0.945	0.971												
13	0.677	0.670	0.661	0.653	0.645	0.646	0.679	0.816	0.904	0.940	0.963	0.983											
14	0.666	0.659	0.649	0.640	0.632	0.634	0.667	0.807	0.903	0.940	0.962	0.975	0.988										
15	0.667	0.657	0.645	0.634	0.624	0.621	0.653	0.801	0.895	0.923	0.951	0.951	0.970	0.980									
16	0.647	0.637	0.625	0.613	0.603	0.601	0.634	0.785	0.879	0.905	0.936	0.933	0.955	0.967	0.996								
17	0.642	0.632	0.620	0.610	0.599	0.601	0.634	0.775	0.862	0.877	0.908	0.913	0.939	0.953	0.984	0.986							
18	0.751	0.743	0.735	0.726	0.718	0.717	0.737	0.852	0.907	0.909	0.924	0.906	0.927	0.931	0.964	0.966	0.966						
19	0.776	0.771	0.764	0.758	0.751	0.751	0.764	0.864	0.896	0.899	0.911	0.901	0.919	0.923	0.948	0.946	0.953	0.985					
20	0.828	0.824	0.816	0.809	0.802	0.800	0.813	0.900	0.913	0.908	0.911	0.895	0.911	0.908	0.933	0.926	0.935	0.979	0.990				
21	0.836	0.832	0.826	0.820	0.813	0.812	0.825	0.904	0.906	0.898	0.902	0.888	0.898	0.891	0.917	0.911	0.921	0.971	0.985	0.995			
22	0.843	0.839	0.832	0.826	0.819	0.818	0.831	0.908	0.909	0.898	0.898	0.880	0.892	0.883	0.910	0.904	0.911	0.969	0.980	0.994	0.997		
23	0.844	0.840	0.832	0.826	0.819	0.818	0.830	0.906	0.906	0.892	0.888	0.866	0.880	0.869	0.898	0.892	0.897	0.962	0.969	0.988	0.988	0.997	
24	0.841	0.836	0.829	0.822	0.815	0.814	0.826	0.900	0.899	0.882	0.873	0.849	0.864	0.852	0.881	0.876	0.878	0.949	0.953	0.976	0.974	0.989	0.997

Table C.10. October Hourly Ambient Temperature Correlations

Hour	1	2	3	4	5	6	7	8	9	10	11	12	13	14	15	16	17	18	19	20	21	22	23
2	0.996																						
3	0.984	0.996																					
4	0.963	0.983	0.996																				
5	0.957	0.978	0.993	0.999																			
6	0.946	0.969	0.986	0.995	0.999																		
7	0.945	0.968	0.984	0.993	0.996	0.997																	
8	0.933	0.957	0.974	0.983	0.986	0.987	0.988																
9	0.902	0.926	0.943	0.952	0.952	0.951	0.950	0.976															
10	0.845	0.867	0.881	0.889	0.890	0.888	0.890	0.925	0.971														
11	0.810	0.828	0.839	0.843	0.844	0.843	0.844	0.884	0.943	0.987													
12	0.788	0.805	0.816	0.819	0.821	0.820	0.820	0.859	0.917	0.971	0.988												
13	0.748	0.766	0.777	0.783	0.782	0.778	0.781	0.816	0.887	0.950	0.963	0.978											
14	0.723	0.734	0.740	0.740	0.740	0.735	0.740	0.770	0.832	0.908	0.924	0.950	0.978										
15	0.708	0.719	0.725	0.725	0.724	0.720	0.725	0.753	0.816	0.897	0.913	0.940	0.970	0.996									
16	0.719	0.731	0.737	0.738	0.737	0.733	0.738	0.765	0.830	0.911	0.926	0.949	0.972	0.992	0.996								
17	0.707	0.724	0.735	0.740	0.740	0.738	0.741	0.770	0.832	0.911	0.920	0.935	0.964	0.978	0.982	0.991							
18	0.704	0.720	0.732	0.738	0.741	0.741	0.743	0.772	0.833	0.905	0.914	0.921	0.951	0.958	0.964	0.977	0.991						
19	0.712	0.727	0.738	0.742	0.745	0.744	0.747	0.774	0.831	0.903	0.908	0.904	0.931	0.940	0.947	0.962	0.981	0.991					
20	0.683	0.704	0.722	0.733	0.735	0.735	0.737	0.768	0.826	0.894	0.895	0.890	0.919	0.926	0.931	0.948	0.974	0.984	0.992				
21	0.651	0.674	0.693	0.707	0.712	0.714	0.716	0.747	0.810	0.876	0.877	0.867	0.901	0.900	0.904	0.925	0.956	0.973	0.985	0.993			
22	0.650	0.673	0.693	0.707	0.711	0.713	0.716	0.745	0.809	0.873	0.873	0.862	0.900	0.898	0.901	0.921	0.954	0.971	0.981	0.989	0.998		
23	0.647	0.671	0.690	0.704	0.708	0.709	0.713	0.741	0.806	0.868	0.866	0.854	0.897	0.892	0.894	0.914	0.948	0.963	0.972	0.980	0.991	0.998	
24	0.639	0.663	0.682	0.696	0.700	0.701	0.706	0.732	0.797	0.857	0.852	0.839	0.886	0.881	0.881	0.900	0.935	0.950	0.958	0.965	0.979	0.990	0.997

Table C.11. November Hourly Ambient Temperature Correlations

Hour	1	2	3	4	5	6	7	8	9	10	11	12	13	14	15	16	17	18	19	20	21	22	23
2	0.999																						
3	0.995	0.999																					
4	0.988	0.995	0.999																				
5	0.984	0.992	0.997	0.999																			
6	0.979	0.988	0.994	0.997	0.999																		
7	0.974	0.983	0.988	0.991	0.993	0.994																	
8	0.967	0.977	0.983	0.987	0.989	0.991	0.997																
9	0.962	0.969	0.973	0.975	0.973	0.969	0.972	0.978															
10	0.914	0.920	0.923	0.924	0.919	0.911	0.913	0.924	0.979														
11	0.862	0.864	0.864	0.862	0.854	0.843	0.845	0.859	0.935	0.985													
12	0.830	0.832	0.831	0.829	0.819	0.808	0.810	0.825	0.903	0.963	0.992												
13	0.806	0.806	0.804	0.801	0.790	0.777	0.778	0.794	0.879	0.947	0.984	0.996											
14	0.789	0.789	0.787	0.783	0.771	0.758	0.758	0.771	0.856	0.925	0.969	0.986	0.992										
15	0.779	0.781	0.780	0.778	0.768	0.755	0.754	0.767	0.852	0.924	0.967	0.985	0.990	0.997									
16	0.771	0.775	0.776	0.775	0.766	0.754	0.753	0.765	0.850	0.920	0.961	0.975	0.978	0.988	0.995								
17	0.796	0.801	0.804	0.804	0.796	0.787	0.787	0.801	0.875	0.934	0.967	0.975	0.976	0.984	0.990	0.996							
18	0.806	0.812	0.815	0.816	0.809	0.801	0.805	0.819	0.886	0.939	0.967	0.974	0.971	0.977	0.982	0.988	0.996						
19	0.805	0.811	0.813	0.814	0.808	0.800	0.804	0.816	0.884	0.935	0.962	0.967	0.964	0.971	0.976	0.984	0.992	0.998					
20	0.779	0.784	0.787	0.788	0.782	0.776	0.787	0.800	0.864	0.916	0.946	0.953	0.946	0.953	0.959	0.968	0.976	0.987	0.991				
21	0.761	0.765	0.768	0.768	0.762	0.756	0.770	0.783	0.846	0.897	0.927	0.935	0.927	0.934	0.939	0.948	0.955	0.969	0.976	0.996			
22	0.755	0.760	0.762	0.762	0.756	0.750	0.765	0.777	0.840	0.891	0.921	0.928	0.920	0.927	0.932	0.941	0.947	0.962	0.970	0.993	0.999		
23	0.749	0.754	0.755	0.755	0.750	0.744	0.759	0.771	0.833	0.884	0.913	0.921	0.912	0.918	0.923	0.932	0.938	0.954	0.963	0.988	0.997	0.999	
24	0.742	0.746	0.748	0.747	0.742	0.736	0.752	0.763	0.825	0.875	0.905	0.912	0.903	0.909	0.913	0.922	0.927	0.945	0.954	0.983	0.994	0.997	0.999

Table C.12. December Hourly Ambient Temperature Correlations

Hour	10	11	12	13	14
11	0.749				
12	0.769	0.914			
13	0.651	0.713	0.823		
14	0.804	0.605	0.706	0.770	
15	0.782	0.843	0.907	0.814	0.682

Table C.13. January Hourly GHI Correlations

Hour	10	11	12	13	14
11	0.737				
12	0.551	0.677			
13	0.385	0.665	0.786		
14	0.530	0.742	0.683	0.735	
15	0.439	0.718	0.744	0.637	0.823

Table C.14. February Hourly GHI Correlations

Hour	9	10	11	12	13	14
10	0.783					
11	0.697	0.931				
12	0.584	0.813	0.913			
13	0.672	0.743	0.814	0.906		
14	0.599	0.751	0.774	0.860	0.882	
15	0.525	0.649	0.639	0.724	0.776	0.944

Table C.15. March Hourly GHI Correlations

Hour	8	9	10	11	12	13	14	15	16
9	0.818								
10	0.706	0.861							
11	0.685	0.770	0.865						
12	0.692	0.686	0.727	0.890					
13	0.625	0.727	0.750	0.802	0.877				
14	0.589	0.629	0.644	0.690	0.794	0.893			
15	0.507	0.645	0.665	0.681	0.723	0.873	0.864		
16	0.465	0.586	0.601	0.634	0.726	0.812	0.862	0.829	
17	0.502	0.638	0.667	0.671	0.688	0.751	0.778	0.800	0.876

Table C.16. April Hourly GHI Correlations

Hour	8	9	10	11	12	13	14	15	16
9	0.849								
10	0.687	0.838							
11	0.562	0.654	0.664						
12	0.448	0.455	0.485	0.883					
13	0.402	0.402	0.416	0.776	0.864				
14	0.294	0.384	0.454	0.635	0.634	0.636			
15	0.100	0.246	0.215	0.487	0.531	0.610	0.229		
16	0.330	0.532	0.438	0.441	0.321	0.373	0.105	0.680	
17	0.148	0.361	0.344	0.305	0.039	0.191	0.277	0.441	0.574

Table C.17. May Hourly GHI Correlations

Hour	7	8	9	10	11	12	13	14	15	16	17
8	0.810										
9	0.696	0.752									
10	0.588	0.650	0.638								
11	0.392	0.387	0.464	0.645							
12	0.352	0.478	0.378	0.674	0.742						
13	0.406	0.505	0.527	0.682	0.682	0.719					
14	0.335	0.419	0.303	0.596	0.523	0.699	0.788				
15	0.036	0.145	0.270	0.393	0.576	0.510	0.784	0.701			
16	0.072	0.173	0.051	0.243	0.367	0.477	0.586	0.672	0.750		
17	0.053	0.165	0.168	0.224	0.406	0.442	0.617	0.729	0.801	0.857	
18	0.101	0.194	0.153	0.324	0.475	0.494	0.640	0.730	0.776	0.882	0.921

Table C.18. June Hourly GHI Correlations

Hour	8	9	10	11	12	13	14	15	16	17
9	0.597									
10	0.752	0.451								
11	0.524	0.518	0.524							
12	0.734	0.338	0.497	0.504						
13	0.712	0.426	0.635	0.721	0.743					
14	0.713	0.375	0.517	0.627	0.740	0.770				
15	0.699	0.412	0.482	0.350	0.770	0.551	0.700			
16	0.428	0.142	0.287	0.407	0.647	0.549	0.689	0.581		
17	0.491	0.234	0.347	0.224	0.612	0.339	0.595	0.757	0.473	
18	0.461	0.228	0.484	0.467	0.450	0.455	0.675	0.369	0.325	0.594

Table C.19. July Hourly GHI Correlations

Hour	8	9	10	11	12	13	14	15	16
9	0.751								
10	0.756	0.797							
11	0.576	0.569	0.606						
12	0.627	0.579	0.698	0.866					
13	0.530	0.523	0.631	0.780	0.809				
14	0.491	0.488	0.533	0.655	0.695	0.755			
15	0.495	0.605	0.614	0.622	0.641	0.616	0.775		
16	0.457	0.426	0.543	0.515	0.587	0.635	0.746	0.534	
17	0.497	0.514	0.518	0.328	0.316	0.296	0.578	0.505	0.654

Table C.20. August Hourly GHI Correlations

Hour	9	10	11	12	13	14	15	16
10	0.859							
11	0.704	0.882						
12	0.702	0.814	0.818					
13	0.716	0.774	0.860	0.732				
14	0.627	0.784	0.860	0.730	0.821			
15	0.592	0.597	0.666	0.679	0.740	0.763		
16	0.604	0.656	0.699	0.641	0.719	0.705	0.783	
17	0.475	0.641	0.697	0.585	0.694	0.826	0.749	0.805

Table C.21. September Hourly GHI Correlations

Hour	9	10	11	12	13	14	15
10	0.867						
11	0.666	0.726					
12	0.567	0.560	0.652				
13	0.605	0.492	0.663	0.678			
14	0.649	0.577	0.646	0.843	0.892		
15	0.616	0.520	0.572	0.756	0.812	0.884	
16	0.532	0.418	0.584	0.569	0.764	0.700	0.732

Table C.22. October Hourly GHI Correlations

Hour	10	11	12	13	14	15
11	0.841					
12	0.866	0.888				
13	0.739	0.774	0.830			
14	0.607	0.646	0.759	0.662		
15	0.665	0.750	0.798	0.740	0.920	
16	0.809	0.740	0.839	0.596	0.820	0.854

Table C.23. November Hourly GHI Correlations

Hour	10	11	12	13	14	15
11	0.883					
12	0.841	0.908				
13	0.801	0.838	0.893			
14	0.747	0.732	0.836	0.810		
15	0.820	0.795	0.835	0.866	0.915	
16	0.674	0.617	0.689	0.773	0.869	0.906

Table C.24. December Hourly GHI Correlations

BIBLIOGRAPHY

Barton, J.P. and Infield, D.G., (2004). "Energy storage and its use with intermittent renewable energy." *IEEE Trans. Energy Convers.*, 19(2), 441-448.

Guggenberger, J.D., Elmore, A.C., and Tischeror, J.L., Crow, M.L. (2012). "Performance prediction of a vanadium redox battery for use in portable, scalable microgrids." *IEEE Transactions on smart Grid*, 3(4), 2109-2116.

Salameh, Z.M., Borowy, B.S., and Amin, A.R.A. (1995). "Photovoltaic module-site matching based on capacity factors." *IEEE Transactions on Energy Convers.*, 10(2), 326-331.

VITA

Kayla Marie Speidel was born to Tim and Deneen Speidel of De Soto, Missouri. She was born in St. Louis, Missouri and attended De Soto High School where she was an active member of the National Honor Society and an officer of Art Club. Kayla enjoys spending time outdoors and loves to practice archery and go hiking. After attending two years at Jefferson College in Hillsboro, Missouri, Kayla transferred to Missouri University of Science and Technology where she graduated with a Bachelor of Science degree in Geological Engineering with honors of Magna Cum Laude in May 2012. During her time at Missouri S&T, Kayla was active in the Association of Environmental and Engineering Geologists and Sigma Gamma Epsilon a National Earth Science Honor Society. She finished her Master's degree in Geological Engineering from the Missouri University of Science and Technology in May of 2015.